International Journal of Environment
Volume: 13 | Issue: 02| April - June| 2024

EISSN: 2706-7939 ISSN: 2077-4508
DOI: 10.36632/ije/2024.13.2.4
Journal homepage: www.curresweb.com
Pages: 52-101

Deterioration of Groundwater Quality in the Area between El Saff and El Khashab Canals, South Giza, Egypt

Yahia R. Gedamy

Hydrogeochemistry Department, Desert Research Center, Cairo, Egypt.

Received:15 Jan. 2024 **Accepted:** 30 Mar. 2024 **Published:** 20 April 2024

ABSTRACT

Groundwater is a major important source of water that is vital for human survival and development. Therefore, any changes in groundwater chemical composition will cause its deterioration and impact on its applicability in drinking, agricultural and industrial processes. So, the objective of this work is the study of the deterioration of the groundwater quality in the area between El Saff and El Khashab canals using the integration between the chemical and microbiological data, remote sensing and GIS techniques, in addition to geochemical modeling, and Piper diagram as well as statistical analyses. A total of 87 and 104 water samples were collected during the two periods 2016 and 2022, respectively, from surface water (irrigation canals "El Khashab, El Hager and Masjid Musi alqabliya canals", and El Saff canal for wastewater) and groundwater (Quaternary and Pliocene aquifers). Chemical analyses were carried out to determine the concentrations of major and minor constituents as well as the trace elements in the collected water samples. Also, microbiological pollutants analyses for some selected surface water and groundwater samples were done. The obtained results revealed that the average values of salinities of El Saff canal for wastewater and irrigation canals water samples in the study area increased from 886 to 2034mg/l and from 843 to 1059mg/l by time from periods 2016 to 2022, respectively. Also, the concentrations of sodium, sulfate and chloride in the irrigation canals water samples increased by time from period 2016 to 2022. The average values of the salinities of the Quaternary and Pliocene groundwater samples ranged from 1588 to 1850mg/l and from 2800 to 3820mg/l during the periods 2016 and 2022, respectively. The average values of calcium, sulfate and chloride concentrations showed an increasing trend during time from 2016 to 2022 for both the Quaternary and Pliocene aquifers, and the direction of the increase followed the same trend of salinity increase. The piper diagrams showed that the Quaternary and Pliocene groundwater samples in the study area that affected by El Saff canal for wastewater increased by time from 2016 to 2022. The geochemical model indicated that the maximum mixing ratios of the wastewater of El Saff canal with the Quaternary and Pliocene groundwater samples ranged from 65% to 66% for the Quaternary aquifer and from 72% to 96% for the Pliocene aquifer in the study area. The average values of nitrate and boron concentrations showed a valuable increasing trend during time from 2016 to 2022 in irrigation canals and for both the Quaternary and Pliocene aquifers. The total and fecal coliforms bacteria count in the surface water and groundwater resources in the study area increased by time from 2016 to 2022. Cluster analysis results cleared that the deteriorated groundwater samples in the study area increased by time from 53% of Quaternary and Pliocene aquifers in period 2016 to 73% in period 2022, respectively. The suitability maps revealed that only 23% and 16% of the groundwater samples in the study area during periods 2016 and 2022, respectively, are suitable for human drinking, and that the suitable groundwater for human drinking decreased by time from 2016 to 2022. Staff diagrams indicated that only 27% and 22% in period 2016, and 19% and 17% in period 2022 of the Quaternary and Pliocene groundwater samples, respectively, are good water for irrigating all types of crops, as well as the good water for irrigation decreased by time from 2016 to 2022. Finally, the chemical and microbiological data, as well as the Piper diagram, geochemical model and cluster analysis results confirmed that the deterioration of the groundwater samples in the study area increased by time from 2016 to 2022.

Keywords: Groundwater deterioration, Anthropogenic activities, Irrigation activities, South Giza.

Corresponding Author: Yahia R. Gedamy, Hydrogeochemistry Department, Desert Research Center, Cairo, Egypt. yahiagedamy2014@yahoo.com

1. Introduction

Groundwater is a major and important source of water that is intensively exploited for drinking, domestic, agricultural and industrial purposes in many parts of the world, which is vital for human survival and development (Li *et al.,* 2018a) and in ecological and environmental construction (Bahir *et al.,* 2020). However, what has made the crisis more difficult is the increasing of pollution and deterioration of the quantities of water available to humans because it is being affected by a multitude of factors, such as evaporation, rock dissolution, ion exchanges, water-rock interactions, anthropogenic activities, fertilizers, industrial pollution, or even excessive water use. Where, the water pollution has become an essential issue, particularly in highly water sensitive regions where the mismanagement of pollutants discharge, have caused severe environmental problems (Yang *et al.,* 2019).

The hydrochemical characteristics are considered as direct factors in the measurements of the quality of groundwater environments (Li *et al.,* 2021). Therefore, any changes in groundwater chemical composition will impact its applicability in drinking, agricultural and industrial processes. So, it must be preserved from pollution and deterioration to face the growing population demand for water. Consequently, groundwater is becoming the alternative essential water resource in many parts of Egypt due to the deficit in water balance (River Nile water) as the increase in population and the extensions of reclaimed lands. Also, it plays a decisive role in agricultural production in arid and semi-arid regions (Xu *et al.,* 2019). One of those parts is the study area, which is situated in Giza governorate in Upper Egypt.

The groundwater in the study area, beside that from the Nile water, it use for drinking, domestic, agricultural and industrial purposes. Where, the groundwater is available from the Quaternary and Pliocene aquifers. Also, the demand for groundwater has increased due to the expansion of land reclamation projects for agriculture in the fringes of the desert in that area. The increase in population and expansion of urbanization in the study area lead to the increase in the human activities like the agricultural and industrial activities that are becoming more intensive and extensive, increasing the risk of groundwater pollution, which in turn leads to the deterioration of groundwater in the study area.

In the current study, to investigate the deterioration of the groundwater, an interdisciplinary approach is presented. This approach involves geomorphological, geological, and hydrogeological settings as well as chemical and microbiological analyses of different water resources. The chosen pilot area for applying this approach (Fig.1) includes a variety of problems related to the existence of El Saff canal for wastewater. Consequently, the investigation of surface and groundwater pollution-related problems is necessary.

To achieve the objective, the following were carried out: 1) collection of surface water samples from El Khashab, El Hager and Masjid Musi alqabliya irrigation canals, and from El Saff canal for wastewater, as well as groundwater samples from the Quaternary and Pliocene aquifers during two periods in 2016 and 2022 years, 2) chemical analysis to determine the concentrations of major and minor constituents as well as trace elements in the collected surface water and groundwater samples from the study area, 3) investigating the chemical characteristics of the surface water in the study area, 4) identifying the factors that influence the chemical characteristics of groundwater and their relative contributions using the spatial distribution of the hydrochemical parameters of groundwater, 5) addressing the integrated role of the hydrochemical processes, agriculture activities, wastewater seepage and urbanization on the deterioration of the groundwater system using Piper diagram, 6) determining the mixing ratios between groundwater and surface water using a geochemical model, 7) identifying the factors affecting both the surface water and groundwater quality and causing their deterioration using the discussion of trace elements concentrations and microbiological pollutants for the collected surface water and groundwater samples as well as the spatial distribution of the pollutants parameters of groundwater, 8) using multivariate analysis (cluster statistical analyses) for the surface water and groundwater to determine their relationships in the study area, 9) evaluating the surface water and groundwater quality in the study area for different purposes, and 10) suggesting solutions for mitigation and remediation from pollution sources to help in the protection of groundwater resources from deterioration at the study area.

Site Description

The study area is a part of the Eastern Desert of Egypt, and it lies nearly 50km to the southeast of Cairo along the eastern side of the River Nile (Giza governorate). It is bounded by latitudes 29° 23′ & 29° 46′ N and longitudes 31° 15′ & 31° 23′ E, and it is bordered by Al-Galala plateau at the East and the River Nile at the West, occupying an area of about 800km^2 (Fig. 1). According to Egypt Census estimations for 2017 and 2023, the total populations of the study area are 790,385 and 883,660 people, respectively.

In the study area, there are three irrigation canals (El Khashab, El Hager and Masjid Musi alqabliya irrigation canals) and El Saff canal for wastewater as well as its several open drains that are present, cutting through the old lands. Where, the groundwater in the study area is presented by two main aquifers (Quaternary and Pliocene aquifers). The main industry in the study area is the clay brick industry. The area includes a few small villages or Kafrs as Arab Abu-Said, Kafr Ad-Dismi and others served by an old and deteriorated sewerage network. Some of the scattered communities and houses dispose of their domestic waste either in private septic tanks (latrines) or directly in El-Khashab canal. The area lies within the arid zone of Egypt, characterized by a dry hot summer and a relatively warm winter. The annual means of daily air temperature, relative humidity, and amount of precipitation are 20°C, 55% and 15mm, respectively (EMA, 1996). The evaporation rates are high, attaining 11.65mm/day (Korany *et al.,* 1997a).

Physical Setting

Topographically, the study area is characterized by low relief and a general slope from south to north and from east to west, i.e., the area has a relatively steep slope in its eastern side and the slope becomes gentle westward (towards the River Nile). The elevation ranges from +980m in the southeastern part to +20m above sea level in the vicinities of the River Nile. It is believed that the existing fault with the NW-SE trend is affecting on the variations of the slope values (Yousef, 2007).

The geomorphological features within the study area are resulted from the effects of arid conditions that caused the retreat of slops and the lowering of land (Said, 1954). According to the works of many authors, from those; Yousef (2007), ElSheikh (2008), El-Sayed *et al.,* (2018), Awad (2019) and El-Gaby (2020), the landforms in the study area consist of two main geomorphologic units (Fig.2); the fluviatile plain (water collectors areas) and the calcareous structural plateau (watersheds areas), (Said, 1962 and 1981). The water collectors' areas are the low land areas that have a good capability to collect, store surface water and increase the infiltration rate to recharge groundwater, while the watersheds areas comprise all the existing high lands that form the most conspicuous land features in the study area, and they play principal roles in recharging the groundwater aquifers. The fluviatile plain comprises young alluvial plain and old alluvial plain. The alluvial plain covers the western portions of the study area, constituting the old agricultural lands. The young alluvial plain occupies the old cultivated lands of the Nile Valley, and it was cutting by some irrigation canals and drains. The old alluvial plain occupies the area between the young alluvial plain and the calcareous structural plateau. Recently, this plain has been reclaimed for agriculture due to its good soil potentiality. Also, it was cut by El Saff canal which is almost running parallel to the Nile River. On the other hand, the calcareous structural plateau is located to the east of the old alluvial plain, where it occupies the eastern boundary of the study area.

Geologically, the study area is complicated due to great changes in facies and geologic structures (Awad, 2019). The study area was affected by the origin and development of the River Nile. The Nile valley offers a suitable environment for accumulating Tertiary and Quaternary sediment (El Gaby, 2020). According to the works of many authors, from those; Yousef (2007), ElSheikh (2008), El-Sayed *et al.,* (2018), Awad (2019) and El Gaby (2020), the study area comprises sedimentary-origin rocks belonging to age ranges from Tertiary to Quaternary (Fig. 3). Tertiary strata are characterized by lime facies with thin clayey sand intercalation where they formed under shallow marine conditions. Tertiary succession is distinguished from base to top into Eocene and Pliocene (Abdel-Daiem, 1971).

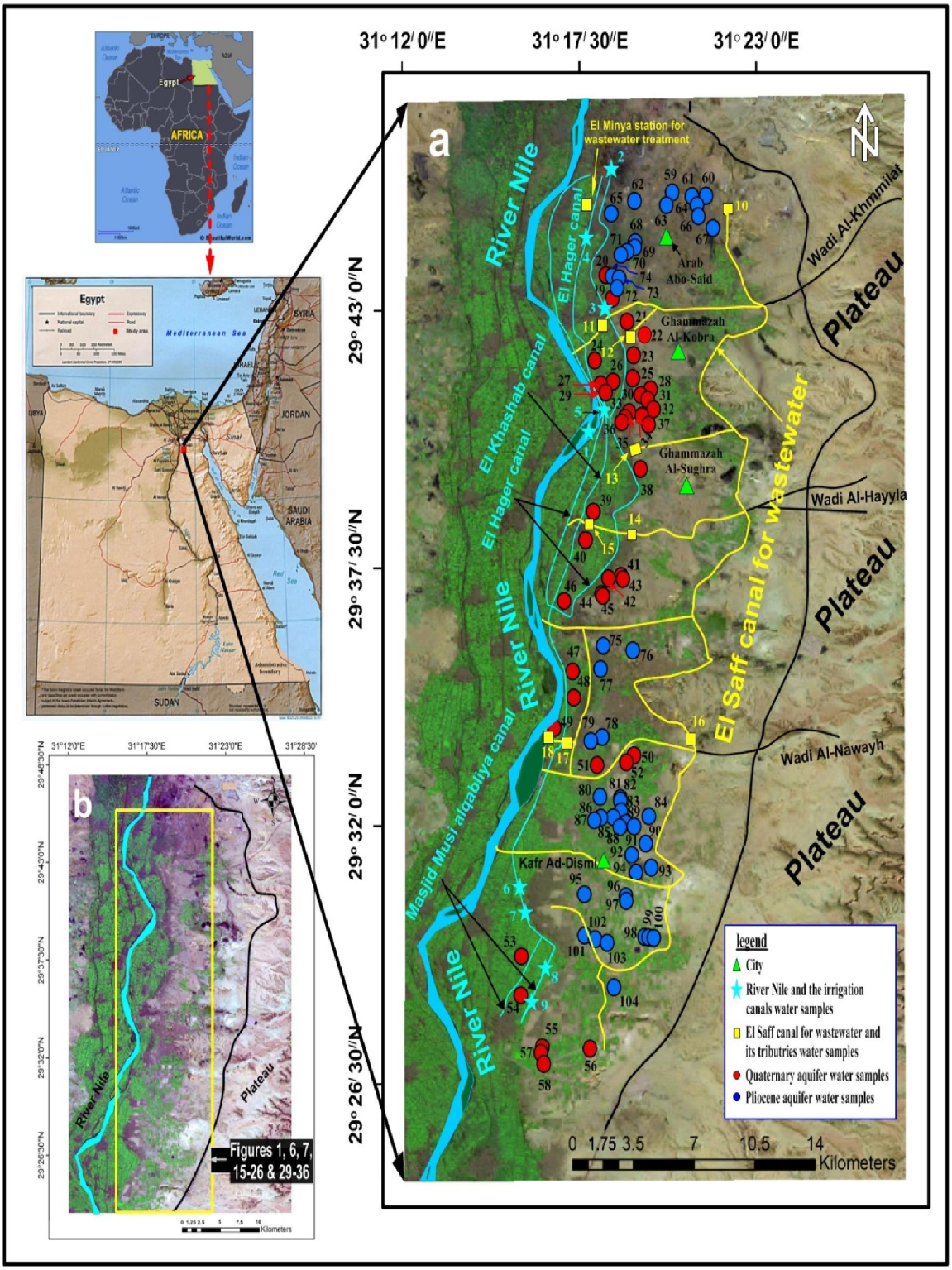

Fig. 1: Key map of the study area; (a) shows the water samples sites map and the irrigation canals and El Saff canal for wastewater, and (b) shows the solid yellow box outlines areas displayed in figures (1, 6, 7, 15-26 and 29-36)

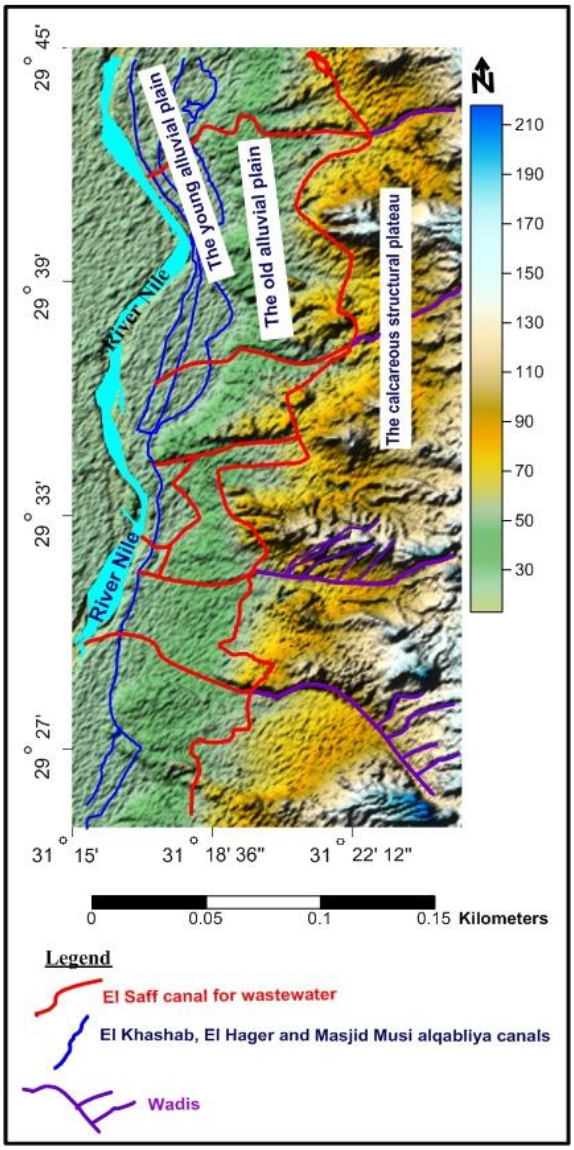

Fig. 2: Landforms map shows the main geomorphological units illustrated over the digital elevation model (DEM)

The Eocene rocks are considered as one of the most prevalent geological outcrops, where they form the eastern structural plateau. The Eocene sediments are composed of carbonates that are occasionally mixed with varying amounts of clastic. The Pliocene deposits consist mainly of weathered fine sand, marly limestone, sandy limestone and sandy marl. These sediments underlie the Pleistocene deposits and unconformably overlie the Eocene rocks (El-Sayed, 1993). The Quaternary sediments occupy the courses of the main wadis, as well as the western part of the study area between the eastern limestone plateau and the Nile channel. These deposits are composed of fluviatile sands and gravels and can be subdivided from base to top into the Pleistocene and Holocene. The Pleistocene strata are deposited under terrestrial conditions (Abdel-Daiem, 1971), where they are formed of clays, marl, sands and gravel (El-Sayed, 1993). The Holocene deposits occupy the flood plain of the Nile valley and consist of Nile silt, clays, sands and gravels (Abdou, 1994).

Water Resources

In the current study, the surface water is represented by the River Nile, and three irrigation canals were dissecting the study area and flowing from south to north (Masjid Musi alqabliya, El Khashab and

El Hager canals), in addition to El Saff canal for wastewater. However, the groundwater is represented by two aquifers (the Quaternary and Pliocene aquifers), Fig. 1.

Surface water resources

The River Nile is responsible for the irrigation of the cultivated lands, either directly or indirectly, through the three irrigation canals. The course of the river within the study area is underlain by the Quaternary deposits (sands and gravels), which in turn are underlain by Pliocene clays (Abdu, 1994). On the other hand, the three irrigation canals transfer the River Nile water to irrigate the old cultivated lands adjacent to the River Nile. Masjid Musi canal irrigates the old cultivated lands between Atfih and El Saff while El Khashab and El Hager canals irrigate the old cultivated lands north of El Saff city to Arab Abu Saed village at the extreme north.

El Saff canal for wastewater is a canal constructed for transporting the treated industrial water and wastewater from Helwan and El Tibbin cities reaching to El Saff-Atfih area. Whereas, El Saff canal receives its water (about 350,000m^3 everyday) through a pumping station located to the east of Arab Abu Saed locality, and it is used to irrigate the newly reclaimed lands in the eastern fringes of the study area that are characterized by ground elevation ranging from +80m to about +30m. Noteworthy to mention that, El Saff canal for wastewater was excavated generally through the Pliocene clay sediments and sometimes it cuts on the foot slope of the eastern limestone plateau and is also traversed by many wadis' courses. Wadi deposits that fill these courses facilitate the arrival of the canal water not only to the old cultivated lands but also to the Nile course itself (ElSheikh, 2008 and El Gaby, 2020).

Groundwater resources

Based on some wells logs data, a geologic map and previous studies, two main aquifers are distinguished in the study area. These are the Quaternary and Pliocene aquifers (Yousef, 2007 and El-Gaby, 2020).

Quaternary aquifer

The Quaternary aquifer resides on the narrow strip adjacent to the River Nile and is located in the western part of the study area. The Quaternary aquifer can be considered as unconfined to semi-confined aquifer due to the presence of semi-pervious clay layer capping the aquifer. The semi-confined condition characterizes the old cultivated lands, while the unconfined condition prevails in the new reclaimed areas where the Quaternary sediments existed on the ground surface (ElSheikh, 2008). The Quaternary aquifer is considered to be of high water potential because its sediments consist of Pleistocene deposits.

The Pleistocene deposits are considered as the main aquifer within the western part of the area. The sediments of the Pleistocene cover some parts north of the study area between the River Nile and the limestone plateau, and they are covered by the Nile deposits in the southern part. The Pleistocene deposits consist mainly of sand and gravels intercalated with lenses of clay (Figs. 4 & 5). The Pleistocene sediments are differentiated into two members, an old-sand gravel member and young clay-silt member. The total thickness of the Pleistocene deposits ranges from 100m at the west adjacent to the River Nile to about a few meters eastward and usually decreases until vanishing near the eastern fringes (Awad, 2019).

The groundwater levels are more than 60m + msl in the eastern parts of the area adjacent to the eastern plateau and decrease westward, reaching less than 18m +msl adjacent to the River Nile (Awad, 2019). Thus, the Quaternary aquifer in the study area could be recharged from different sources, including leakage from the irrigation canals, excess irrigation water, and drained wastewater (El Saff canal for wastewater) from the populated and industrial areas (Awad, 2019) as well as from the recent and old Nile floods (ElSheikh, 2008). Korany *et al.,* (1997a) suggested that the Quaternary aquifer in the study area was partially recharged from surface runoff during occasional rainstorms in winter at the eastern drainage basins. Also, Yousef (2007) reported that the Quaternary aquifer was mainly recharged from the deep Nubian Sandstone aquifer through the N-W active fault systems.

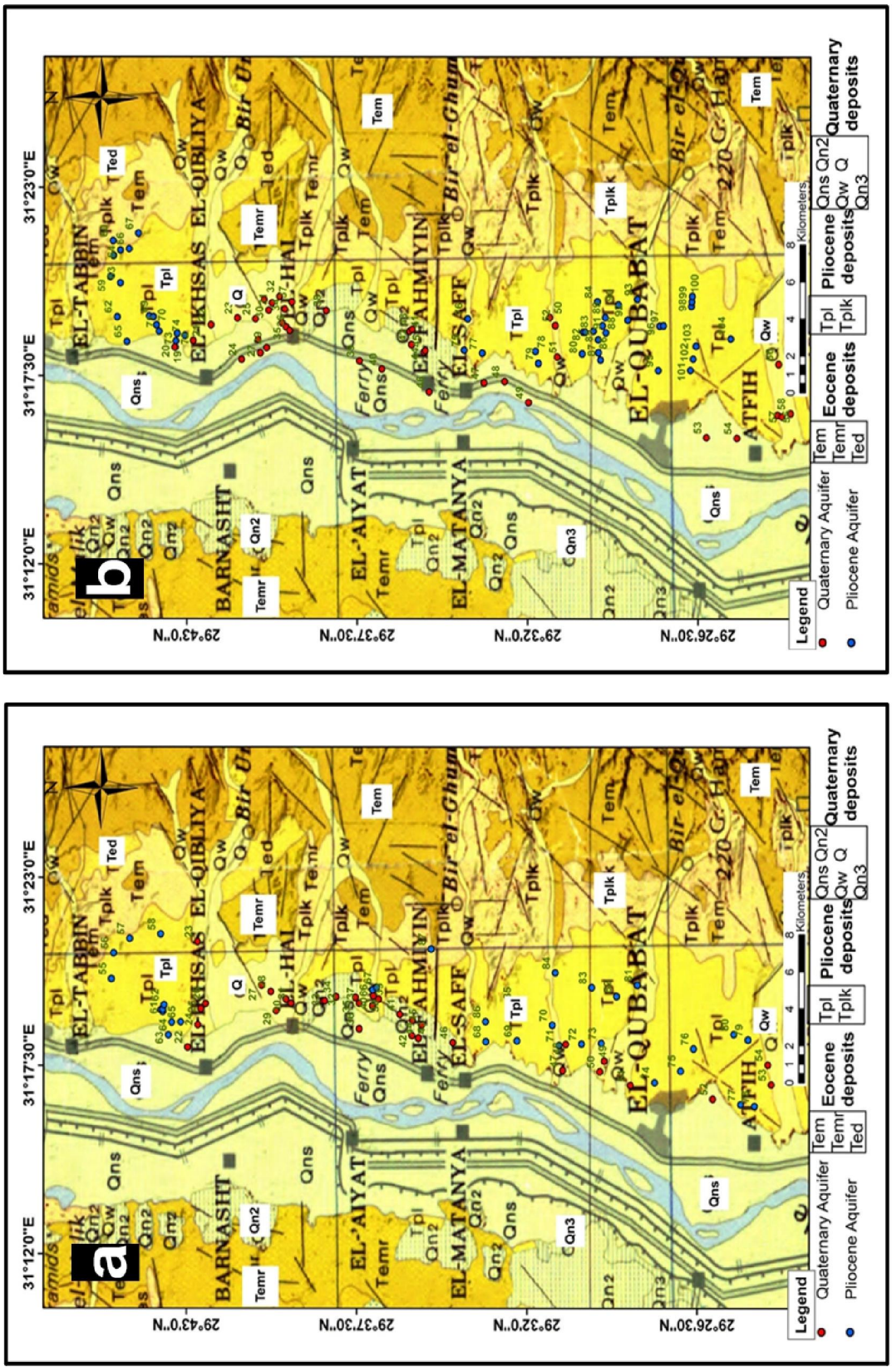

Fig.3 The geological map of the study area signed on it the sites of the groundwater samples in a (Period, 2016) and b (Period, 2022) (After CONOCO, 1987)

Tertiary aquifers (Pliocene aquifer)

The Pliocene aquifer consists of fine to medium sands, clays, calcareous and argillaceous sediments. The groundwater is generally occurs under unconfined conditions (El Gaby, 2020). The Pliocene aquifer is recharged by the downward seepage from irrigation canals and drains where their water level is higher than that of the Quaternary aquifer and the River Nile. On the other hand, the upward leakage from the fractured Eocene aquifer contributes in the Pliocene aquifer recharge (Abdou, 1994). Also, this aquifer is recharged through the deep active N-W fault systems (Yousef, 2007). In addition, it is recharged from the ancient and recent floods (ElSheikh, 2008), Figs. (4 & 5).

In general, in the study area, the aquifers are hydraulically connected with each other through faults, fissures and cracks that dominate the surface and subsurface of the region (Yousef, 2007 and El-Sayed *et al.,* 2018), Figs. (4 & 5).

The groundwater flow direction in the study area is westwards to the River Nile (El Gaby, 2020), i.e., the movement of groundwater takes place essentially from east to west, from the new reclaimed area around El Saff canal (+71m) to the old cultivated lands (+26m to +24m) near the River Nile (+23m) since the latter acts as a discharging area for the former. Another flow of groundwater from south to north, which coincides with the general flow of surface water in the main irrigation canals is recorded (ElSheikh, 2008).

The depth to water for the Quaternary aquifer ranges from 6 to 35m while for the Pliocene aquifer it ranges from 7 to 40m (El Gaby, 2020). The depths to water levels (from the ground surface) in the wells in the study area vary from site to site according to the topographic elevations.

2. Materials and Methods

Water sampling

Two field trips were carried out during the years 2016 and 2022, respectively, as a part of the geological, hydrogeological and hydrogeochemical investigations of the study area. A total of 87 and 104 water samples were collected during the two periods, respectively, from the surface water (irrigation canals "El Khashab, El Hager and Masjid Musi alqabliya canals", and El Saff canal for wastewater) and the groundwater (Quaternary and Pliocene aquifers) to investigate the deterioration of the groundwater in the study area. The first trip (2016) was accomplished by collecting 21 surface water and 66 groundwater samples, while the second trip (2022) was accomplished by collecting 18 surface water and 86 groundwater samples. The locations (longitudes and latitudes) of the collected water samples were identified using a Global Positioning System (GPS) model etrex 10 (German) and therefore plotted to generate the map of the sampling locations (Fig. 1). The water samples were collected in new, tightly capped 500ml polyethylene sterile bottles that were rinsed three to four times with the water sample before filling them to capacity and then labeled accordingly. The groundwater samples were collected from water wells after pumping water for 10-15min to minimize errors due to oxidizing and carbonating agents. The temperature, electrical conductivity (EC) and potential of hydrogen ion concentration (pH) were determined immediately after the collection of the samples using a portable electrical conductivity meter (Jenway, model 470) and a pH meter (Jenway, model 3150). Before each measurement, the pH meter was calibrated with a reference buffer solution of pH=4. The available hydrogeological data (depth to water, total well depth, lithology, and the water-bearing formations), as well as the geological information, were identified during the field trip.

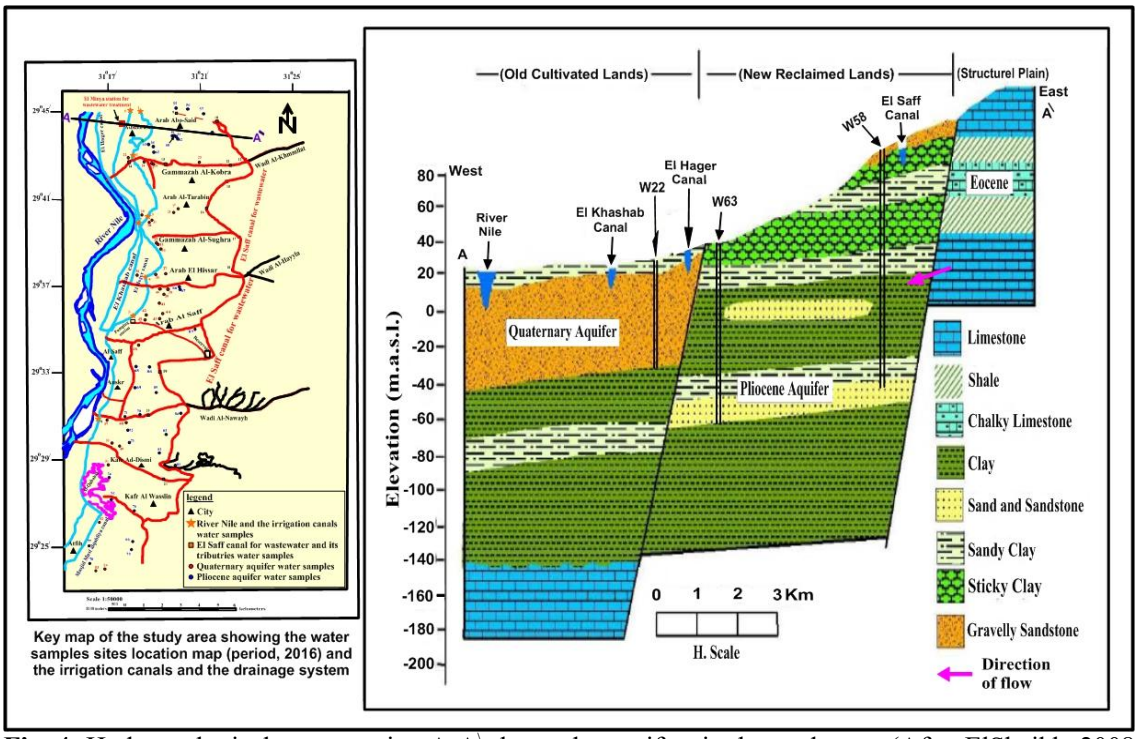

Fig. 4: Hydrogeological cross-section A-A\ shows the aquifers in the study area (After ElSheikh, 2008 and El Gaby, 2020).

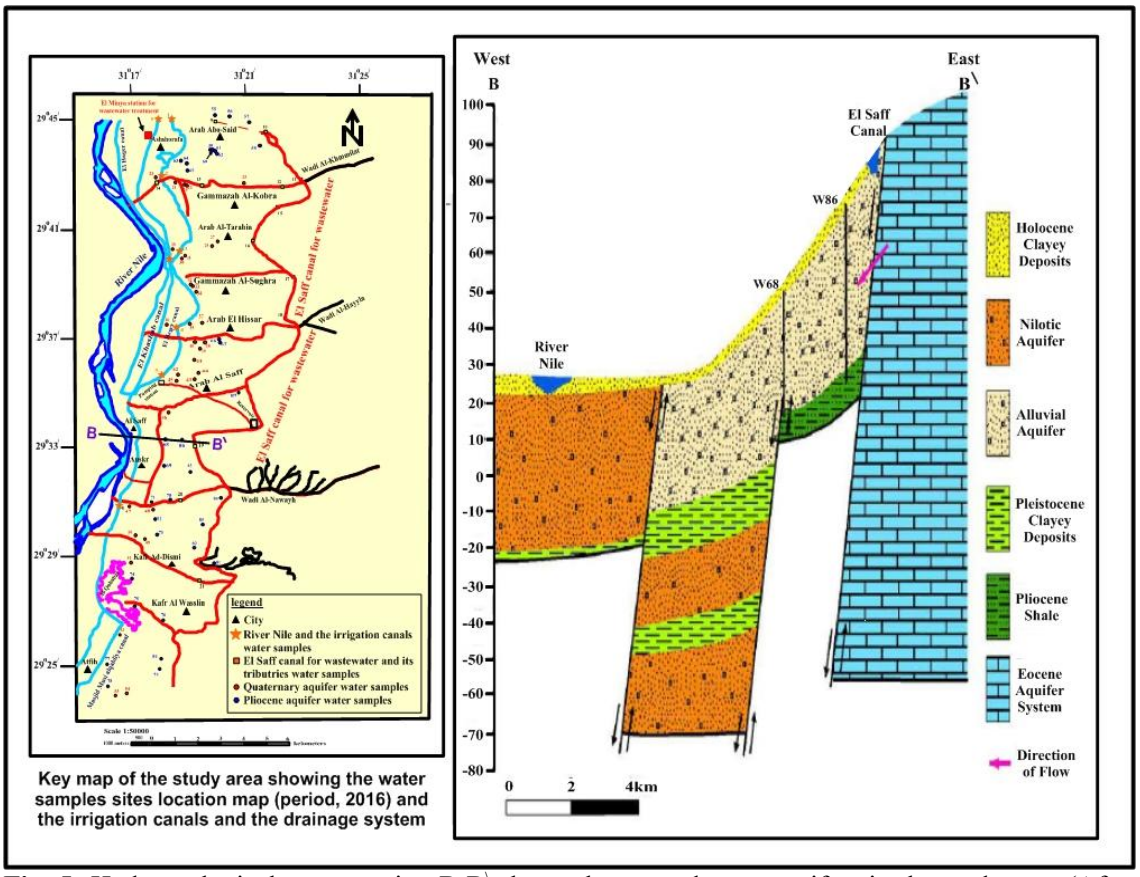

Fig. 5: Hydrogeological cross-section B-B\ shows the groundwater aquifers in the study area (After Youssef, 2007; ElSheikh, 2008 and El Gaby, 2020)

Analytical techniques

The collected water samples were tightly packed to protect them from atmospheric CO_2, transported to the laboratory and stored in a refrigerator at 4°C before analysis. The extra-pure analytical-grade reagents and chemical standards (Merck Grade) were used for the groundwater quality analysis by adopting standard procedures. The collected water samples were divided into three portions to be analyzed by the author; the first portion was taken in a special container (100ml) for the measurement of major cations and anions according to Rainwater and Thatcher (1960). The second portion was taken in another special container (100ml) for the measurement of minor constituents according to Fishman and Friedman (1985). The third portion was acidified with nitric acid (1%) and stored in pre-cleaned polyethylene bottles for the measurement of trace elements according to the methods adopted by American Society for Testing and Materials (ASTM, 2002). Finally, representative surface water and groundwater samples were collected in sterile bottles to recognize the total and fecal coliform bacteria as an indicator of potential bacterial contamination according to the standards methods adopted by American Public Health Association (APHA, 1998).

The collected surface water and groundwater samples were transported to the laboratories of the hydrogeochemistry department at the Desert Research Center, Cairo, Egypt, to carry out the required chemical analyses. Total dissolved solids (TDS) were measured by the calculation method. The analysis of the major elements as sodium (Na^+), potassium (K^+), calcium (Ca^{2+}), magnesium (Mg^{2+}), chloride (Cl^-) and sulfate (SO_4^{2-}) as well as minor constituents as nitrate (NO_3^-) was carried out using an Ion Chromatography device (DIONEX ICS-1100). While carbonate (CO_3^{2-}) and bicarbonate (HCO_3^-) were determined by titration using H_2SO_4. Trace element contents (Al, Cr, Cu, Fe, Mn, Ni, Zn and Pb) as well as minor constituent as boron (B) in the water samples were determined using inductively coupled plasma (ICP). Blank, standards and triplicate samples were run during the analysis of the samples to check the accuracy and reliability of the analysis methods. The number of total and fecal coliforms was determined using the Most Probable Number (MPN) index and MacConkey broth media. The positive tubes were streaked on the Eosin Methylene Blue (EMB) agar plates. Microscopic examination was carried out to ensure gram-negative, non-spore forming rods (APHA, 1998). MPN of fecal streptococci was determined using azide dextrose broth at 37°C for 48hr. Positive tubes were indicated by dense turbidity and confirmed using ethyl violet azide dextrose broth incubated at 37°C for 24hr. (APHA, 1998). Nine multiple tube dilution technique using double and single strength Bromo-Cresol Purple MacConkey medium for detection of *E.coli* (Thermotolerant coliform, TTC) with the production of yellow colored colonies on a membrane filter at 44.5^0C.

Data analysis methods

The obtained chemical data were expressed in milligram per liter (mg/l) or part per million (ppm). It is worth mentioning that, the analytical precision for the measured major ions is about ±5%. Collection of the geomorphological, geological and hydrogeological data of the study area from the previous works and internal reports, and use of a topographic map (scale 1: 100,000) for preparation of the base map of the studied area as well as preparing all the graphical representations and maps for the analytical results through using some computer programs such as Word and Excel 2007 for windows and surfer (v.13) as well as remote sensing and GIS techniques were done. Use of geological maps to sign the collected groundwater samples from the study area on these maps to separate the different aquifers in the study area due to the difficulty of the hydrogeological situation in the study area. All obtained data was tabulated in tables (1, 2, 3, 4, 7, 8, 9, 10, 11 & 12).

Multivariate statistical analysis

In the current study, cluster analysis is used as a statistical method for processing the chemical data of water samples. The method involves working through organizing the items into groups or clusters based on the base of the closely associated they are. The cluster analysis is applied for selected analyses that refer to water chemistry and pollution existence that include; TDS, Ca^{2+}, Mg^{2+}, Na^+, HCO_3^-, SO_4^{2-}, Cl^-, Al, Cr, Cu, Fe, Mn, Ni, Zn, Pb, V, B and NO_3^-. The cluster classification was performed using the SPSS software (v.26), where the hierarchical arrangement is applied, and the data was represented through a dendrogram diagram using the Ward method (Ward, 1963).

Geochemical modeling

The obtained data from the chemical analyses of major and minor constituents as well as trace elements are used as input data for the geochemical modeling using NETPATH. The software package NETPATH for windows (El Kadi *et al.,* 2010), is used to evaluate the subsurface geochemical processes and to provide an indication of the reaction potential of the system, also it is used to perform a variety of aqueous geochemical calculations including the testing of water mixing models, i.e., the NETPATH is a computer program for simulating chemical reactions and transport processes in natural or polluted water. The program is based on the equilibrium chemistry of aqueous solutions interacting with minerals, gases, solid solutions, exchangers, and sorption surfaces.

3. Results and Discussion

Monitoring of changes detection with anthropogenic activities

The change detection over the study area through monitoring of satellite images from 1992 to 2022 (Fig. 6) indicates changes in some features as follows;

1- The digging of El Saff canal for wastewater began in 1982 and was completed in 1987.
2- El Saff canal for wastewater was opened in 1992, and its situation developed until it reached the current situation, and also it is still flowing till now.
3- The anthropogenic activities are in continuous increasing since 1992 till present.
4- The establishment of El Saff canal and the increase of anthropogenic activities has led to huge pressure on groundwater source and caused its contamination.
5- The dire need of water for agricultural activities led to random drilling and over-pumping of groundwater. Consequently, the water chemistry has been affected.
6- The continuous disposal of the wastewater in El Saff canal since 1992 till now led to flowing of the wastewater overflow along the drainage network at the study area, which consequently can be infiltrated into the groundwater.

Structural lineaments extraction

The careful analyses of the structural lineaments clarify the existence of three sets with different trends (E-W, NW-SE and NE-SW), (Fig. 7). The lineament may be geomorphological or tonal (caused by contrast differences) surface features. These linear features represent the weakness zones or structural displacement in Earth's crust (Hobbs, 1904 and 1912). The lineaments analysis suggests that most of lineaments are homogeneously distributed over the area. Also, there are connections between El Saff canal for wastewater and both the Quaternary and Pliocene aquifers. These lineaments are expected to provide a chance for groundwater recharge from different surface water resources.

Hydrochemical characteristics

In the study area, hydrochemical characteristics of the surface water (irrigation canals as well as El Saff canal for wastewater) and groundwater can be discussed through the chemistry of them based on the chemical analyses of pH, electrical conductivity (EC), total dissolved solids (TDS), as well as analytical data of the major ions composition in surface water and groundwater samples (tables 1, 2, 3 & 4).

Surface water chemistry

The surface water in the study area is represented by El Saff canal for wastewater, and three irrigation canals flow from south to north (Masjid Musi alqabliya, El Khashab and El Hager canals). The results of the chemical analyses are shown in tables (1 & 2), and the concentrations of important chemical constituents are presented in box and whisker plots (Figs. 8, 9, 10 & 11). As in tables (1 & 2) and Figs. (8 & 9), the electrical conductivity of the wastewater in El Saff canal in periods (2016 and 2022) ranges from 439 to 3310µS/cm and 1580 to 5500µS/cm with average values of 1495 and 3413µS/cm, respectively. The large variations in EC values are mainly attributed to anthropogenic activities and evaporation processes.

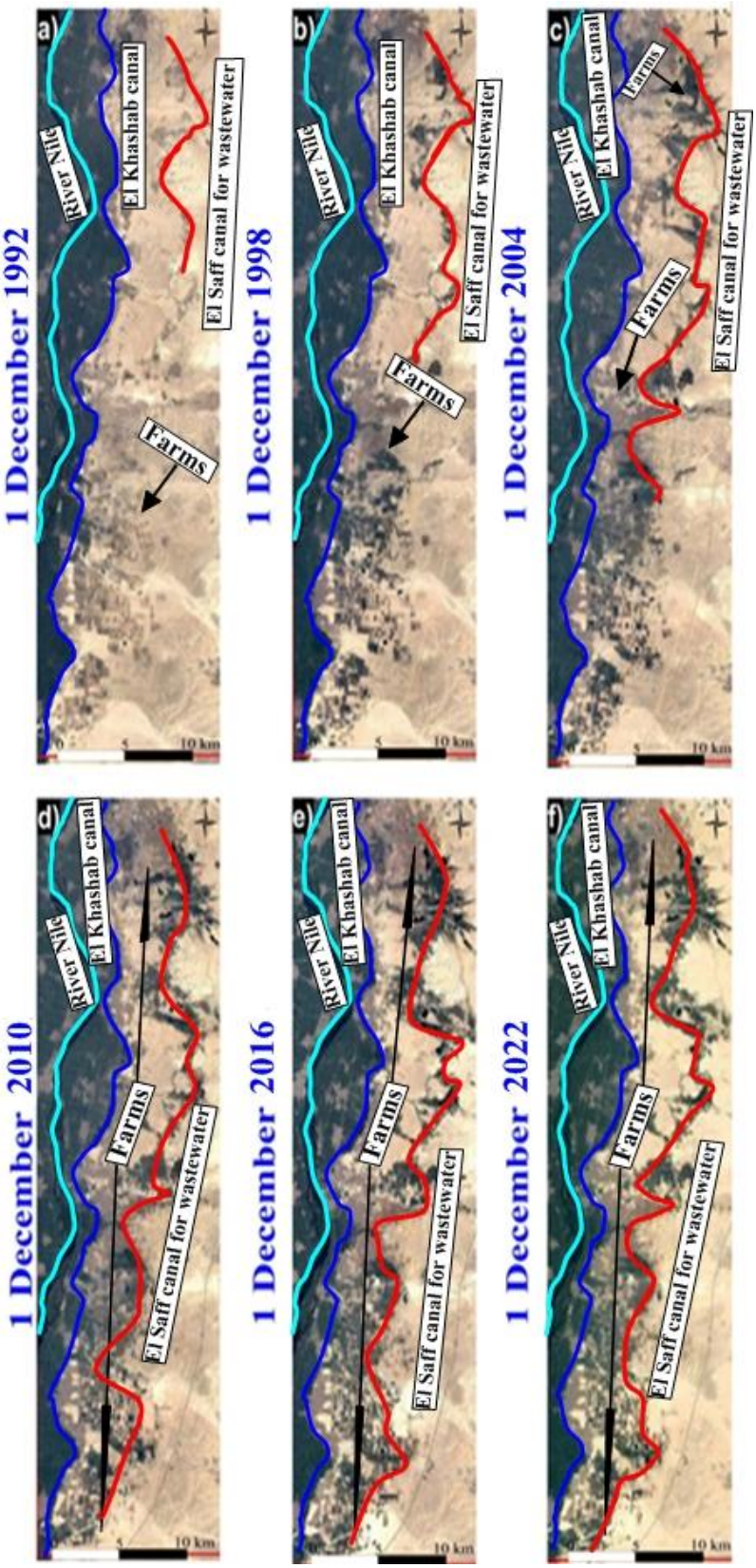

Fig. 6: The monitoring of change detection in the study area using satellites images from 1992 to 2022.

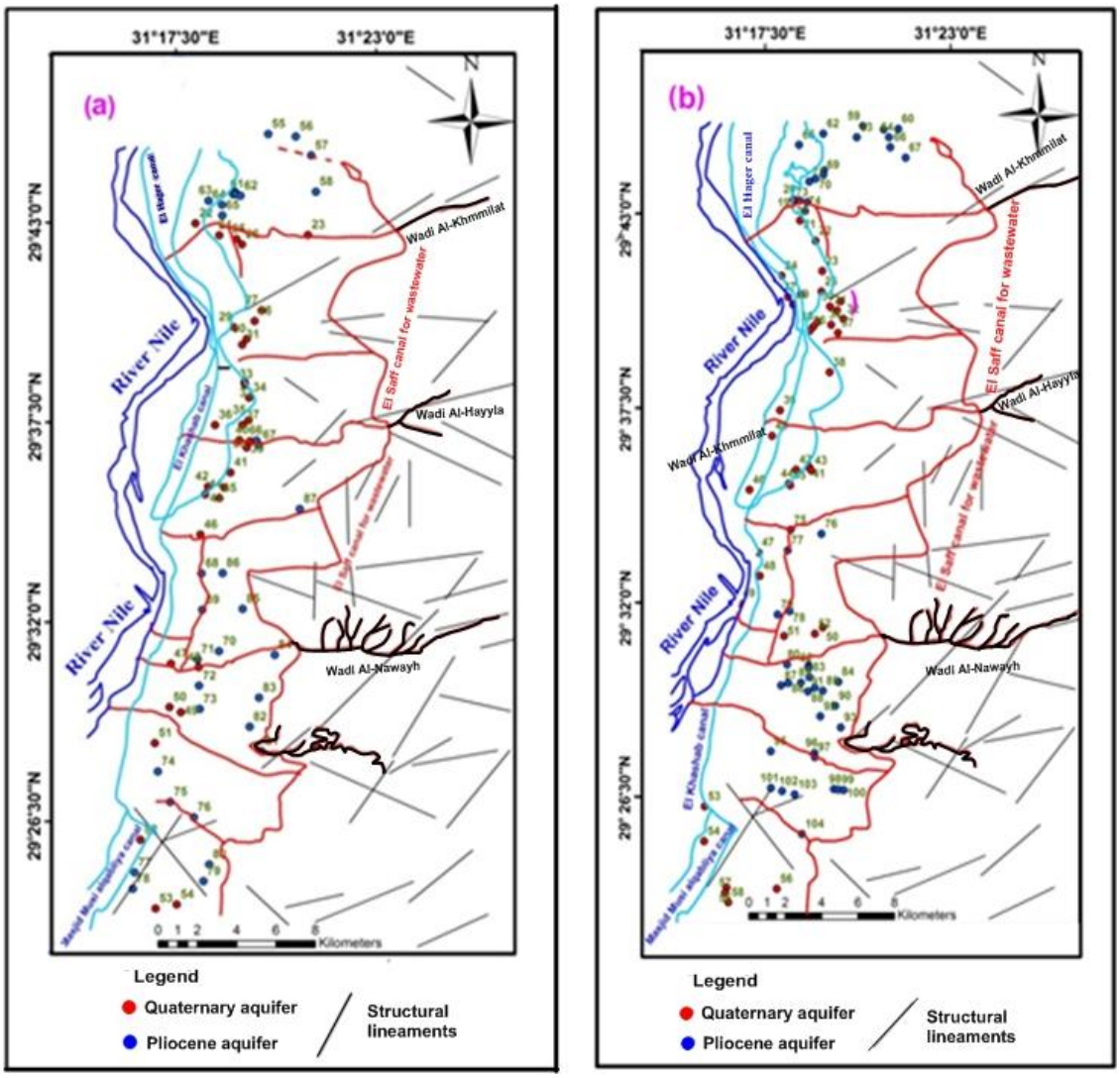

Fig. 7: Extracted structural photo-geological lineaments (faults and/or joints) maps of the study area with the location of groundwater samples in a (period, 2016) and b (period, 2022)

The spatial distribution diagrams of TDS (Figs. 8 & 9) also show similar type variations like EC, and the salinity values of the wastewater in El Saff canal in periods (2016 and 2022) vary from 281 to 1954mg/l and 921 to 3061mg/l with average values of 886 and 2034mg/l, respectively (tables 1 & 2). Also, it was noticed from the tables (1 & 2) and Figs.(8 & 9) that the salinity increased from period 2016 to period 2022. This may be due to the amounts of wastewater, polluted materials, harmful chemicals and garbage that are thrown from factories, agricultural lands and cities into El Saff canal for wastewater. As well as, the canal was generally dug in the Pliocene clay sediments and sometimes cutting the foot slope of the eastern limestone plateau.

As in tables (1 & 2) and Figs.(10 & 11), the pH values of the irrigation canals water samples (period, 2016) and (period, 2022) range from 7.43 to 8.19 with an average value of 7.87, and from 7.2 to 7.5 with an average value of 7.43, respectively, which is weakly alkaline. The EC values of the irrigation canals water samples in periods 2016 and 2022 range between 327 and 4850µS/cm with an average value of 1463µS/cm, and from 560 to 4050µS/cm with an average value of 1660µS/cm, respectively. It is noticed that, the EC values increased from south to north direction (tables 1 & 2) and (Figs. 12 & 13), i.e., from Masjid Musi alqabliya canal to El Hager canal, and the large variations in EC of the irrigation canals water samples in periods (2016 & 2022) are mainly attributed to anthropogenic activities.

The total dissolved solids (TDS) values of the irrigation canals water samples in the study area (period, 2016) and (period, 2022) vary between 150 and 2715mg/l (El Hager canal) with an average value of 843mg/l, and from 281mg/l (Masjid Musi alqabliya canal) to 3018mg/l (El Hager canal) with an average value of 1059mg/l, respectively. 75% and 62% of the irrigation canals water samples (period, 2016) and (period, 2022), respectively, are fresh water, while the rest of samples (25% & 38%) were considered as brackish water. The salinity of the irrigation canals water increased from south to north and it is generally higher at the north than at the south. However, it shows slight fluctuation along its course in accordance with the direction of the water movement (Figs. 12 & 13) and this relatively high salinity is due to the effects of location, direction of water movement, type of soil, type of mixing source and rate of evaporation, as well as the drainage of El Saff canal for wastewater into the River Nile as in El Ghammazah area (Fig.14a), which in turn moves again to the canals, and finally, in some areas, the irrigation canals are used as a drain. Also, it is obvious that the increase of salinity in the irrigation canals water in period (2022) is greater than that in period (2016), (Figs. 12 & 13), which indicates that the deterioration factors as previously mentioned in the former paragraph, increase with time.

The content of calcium in the irrigation canals water samples during periods (2016) and (2022) ranges between 26.39 and 142.13mg/l with an average value of 53.33mg/l, and from 41.67 to 195.83mg/l with an average value of 99.48mg/l, respectively. While magnesium concentration during periods (2016) and (2022) ranges between 14.8 and 133.2mg/l with an average value of 45.18mg/l, and between 10.13 and 111.37mg/l with an average value of 38.1mg/l, respectively. Also, sodium concentration during periods (2016) and (2022) ranges from 23 to 804mg/l with an average value of 208.9mg/l, and from 31 to 833mg/l with an average value of 228.69mg/l, respectively.

HCO_3^- concentration in the irrigation canals water samples in periods (2016) and (2022) varies from 145.31 to 815.3mg/l and 163 to 282mg/l with average values of 270.53 and 190.1mg/l, respectively. While sulfate concentration ranges from 15 to 657mg/l and 48 to 1210mg/l with average values of 129.76 and 311.85mg/l during the periods 2016 and 2022, respectively. Also, chloride concentration in the two periods (2016) and (2022) varies from 14.79 to 971.63mg/l and 33.98 to 690.37mg/l with average values of 259.4 and 277.12mg/l, respectively.

The high concentrations of both sodium, sulfate and chloride in the irrigation canals especially El Hager canal are due to the contamination of the irrigation canals from El Saff canal for wastewater, human activities, and industrial wastes. As in Figs.(10 & 11) and from the average ion concentrations, the main anion in period (2016) was determined by HCO_3^-, followed by Cl^- and SO_4^{2-}, while in period (2022) the main anions were determined by SO_4^{2-}, followed by HCO_3^- and Cl^-. This means that the irrigation canals water was contaminated (deteriorated) by time from 2016 to 2022 as it changed from a less advanced stage dominated by HCO_3^- to an intermediate stage dominated by SO_4^{2-}, respectively.

Groundwater chemistry

The groundwater chemistry in the study area was studied by discussing the pH, salinity, and major ions as follows:

The pH reflects the quality and geochemical equilibrium of the aqueous solution (Hem, 1993). In the study area, it is clear that the pH values of the Quaternary and Pliocene groundwater samples are alkaline, whereas the Quaternary groundwater samples have pH values ranging between 7.02 and 8.32 with an average value of 7.82, and between 7.16 and 8.9 with an average value of 7.83 during the periods 2016 and 2022, respectively (tables 3 & 4). While the Pliocene groundwater samples have pH values ranging between 7.11 and 8.08 with an average value of 7.71, and between 7.03 and 8.64 with an average value of 7.79 during the periods 2016 and 2022, respectively (tables 3 & 4). It can be seen that the pH is relatively stable and is always more than 7.02 without obvious variation, i.e., the groundwater samples are in their natural state.

Table 1: The electrical conductivity (µS/cm) at 25^0C, pH, salinity, and major cations and anions concentrations in the surface water samples as mg/l (Period, 2016)

Statistics	Parameters										
	EC	**pH**	**TDS**	**Ca^{2+}**	**Mg^{2+}**	**Na^{+}**	**K^{+}**	**CO_3^{2-}**	**HCO_3^{-}**	**SO_4^{2-}**	**Cl^{-}**
El Saff canal for wastewater											
Minimum	439	7.00	281	40.1	3	22.1	3.9	16.44	122.1	15	14.79
Maximum	3310	7.64	1954	203	83.88	380	21	20.55	401.14	460	656.4
Average	1495	7.3	886	93.44	34.427	169.06	14.931	11.495	284.717	151.708	249.91
Irrigation canals											
Minimum	327	7.43	150	26.39	14.8	20.5	2.5	8.22	137.09	15	14.79
Maximum	4850	8.19	2715	142.13	133.2	720	84	174	641.26	657	971.63
Average	1463	7.87	843	53.33	45.18	193.29	15.63	41.12	229.41	129.76	259.4

Table 2: The electrical conductivity (µS/cm) at 25^0C, pH, salinity, and major cations and anions concentrations in the surface water samples as mg/l (Period, 2022)

Statistics	Parameters										
	EC	**pH**	**TDS**	**Ca^{2+}**	**Mg^{2+}**	**Na^{+}**	**K^{+}**	**CO_3^{2-}**	**HCO_3^{-}**	**SO_4^{2-}**	**Cl^{-}**
El Saff canal for wastewater											
Minimum	1580	7.05	921	83.33	30.37	155	9.2	8.46	60.21	231.4	306.21
Maximum	5500	7.6	3061	483.32	126.56	575	24	25.38	240.83	1143.9	1057.81
Average	3413	7.20	2034	230.09	74.53	362.5	14.91	14.1	144.78	600.69	664.97
Irrigation canals											
Minimum	560	7.2	281	41.67	10.13	28	3	8.46	154.97	48	33.98
Maximum	4050	7.5	3018	195.83	111.37	800	33	50.76	232.23	1210	690.37
Average	1660	7.43	1059	99.48	38.1	215.63	13.06	15.86	174.19	311.85	277.12

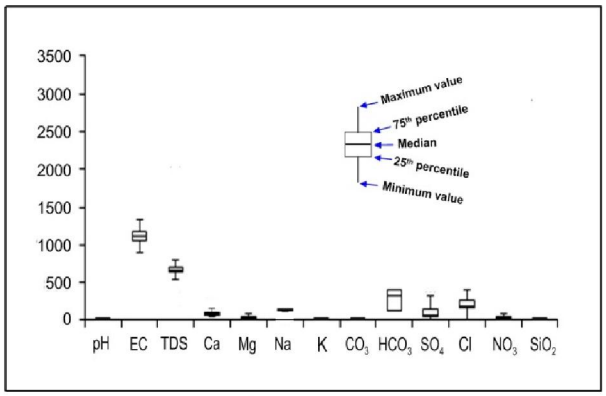

Fig.8 Box plots of pH, EC, TDS and the major ions concentrations in the wastewater of El Saff canal at the study area (period, 2016)

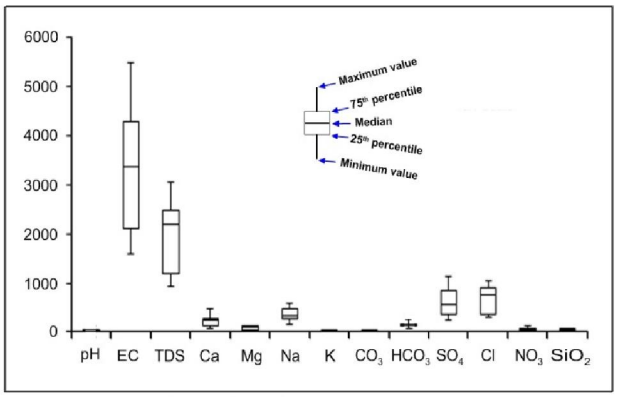

Fig.9 Box plots of pH, EC, TDS and the major ions concentrations in the wastewater of El Saff canal at the study area (period, 2022)

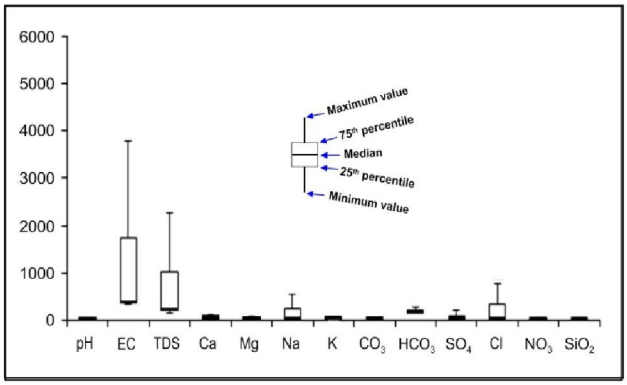

Fig.10 Boxplot of pH, EC, TDS and the major ions concentrations of the irrigation canals water at the study area (Period, 2016)

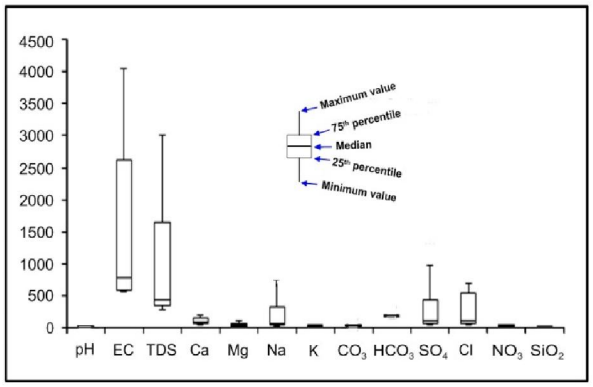

Fig.11 Boxplot of pH, EC, TDS and the major ions concentrations of the irrigation canals water at the study area (Period, 2022)

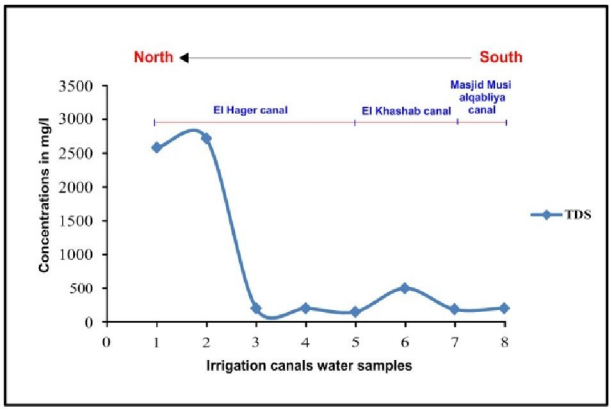

Fig.12 The total dissolved solids in the irrigation canals water (Period, 2016)

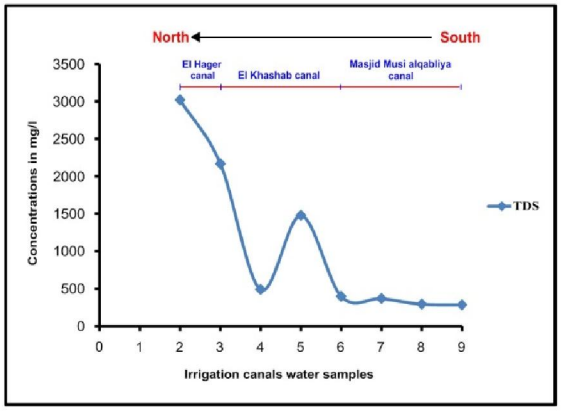

Fig.13 The total dissolved solids in the irrigation canals water (Period, 2022)

Fig. 14: Field photographs showing a) the mixing between the wastewater of El Saff canal and the River Nile, b) El Saff canal for wastewater, c) El Hager canal, d) El Khashab canal and e) Masjid Musi alqabliya canal

According to Chebotarev (1955), most of the groundwater samples of the Quaternary aquifer (52%) during the period (2016) are fresh water (TDS up to 1500mg/l) and the rest of the groundwater samples (48%) are brackish water (TDS 1500-5000mg/l), while during the period (2022) most of the groundwater samples (52%) are brackish water and the rest of the groundwater samples (48%) are fresh water. The total salinity of the Quaternary groundwater samples ranges between 198 and 3856mg/l with an average value of 1587.52mg/l, and between 449 and 4954mg/l with an average value of 1850.45mg/l during the periods 2016 and 2022, respectively (tables 3 & 4), showing a significant increase in the TDS concentrations in the study area by time from 2016 to 2022.

Most of the groundwater samples of the Pliocene aquifer (52%) are brackish water, 33% of the groundwater samples are fresh water and the rest of the groundwater samples (15%) are saline water during the period 2016. While, during period 2022, most of the groundwater samples of the Pliocene aquifer (68%) are brackish water, 17% of the groundwater samples are fresh water and the rest of the groundwater samples (15%) are saline water. The total salinity of the Pliocene groundwater samples ranges between 836 and 11766mg/l with an average value of 2800.48mg/l, and between 603 and 13578mg/l with an average value of 3820.43mg/l during the periods 2016 and 2022, respectively, showing a significant increase in the TDS concentrations in the study area (tables 3 & 4).

It is clear that the total salinity of the groundwater samples of the Quaternary and Pliocene aquifers in the study area increased from period (2016) to period (2022), and the direction of salinity increased eastward (tables 3 & 4) and (Figs. 15a, 15b, 16a & 16b).

The groundwater salinity of the Quaternary and Pliocene aquifers in the concerned area showed many variations, including the following:

The Quaternary aquifer contains fresh water and slightly brackish water. Where the total dissolved solids vary between fresh water in the old cultivated lands at the west of the study area and slightly brackish water in some wells in the new reclaimed lands at the east of the study area. The decrease in salinity is due to the recharge from the irrigation canals, while the slight increase may be due to mixing with brackish water resulted from upward leakage from the Pliocene aquifer, the effect of seepage of El Saff canal for wastewater through faults and clastics (anthropogenic activity), (Fig. 7), as well as return flow after irrigation.

The Pliocene aquifer contains fresh water, brackish water and saline water. This may be due to the fact that, the Pliocene clay encloses pockets of water bearing sandy layers containing considerable amounts of brackish to saline water (3000 - 5000mg/l) and high saline water in some hand dug wells (10000mg/l) that are used in the brick industry, in addition to the over pumping, agricultural activities, seepage of El Saff canal for wastewater through faults and clastics (anthropogenic activity), (Fig. 7). Also, the interaction between the groundwater and the geological formations, the leaching of soil processes and the ion exchange processes that occurred on the clay surface constitute the main cause of the high salinity. Whereas, the presence of some wells with fresh water on the eastern side of the study area is due to the recharge from the irrigation canals.

In general, the groundwater salinity in the study area increased by time from period (2016) to period (2022) due to some factors such as anthropogenic activity, return flow after irrigation and over pumping (Figs. 15a, 15b, 16a & 16b).

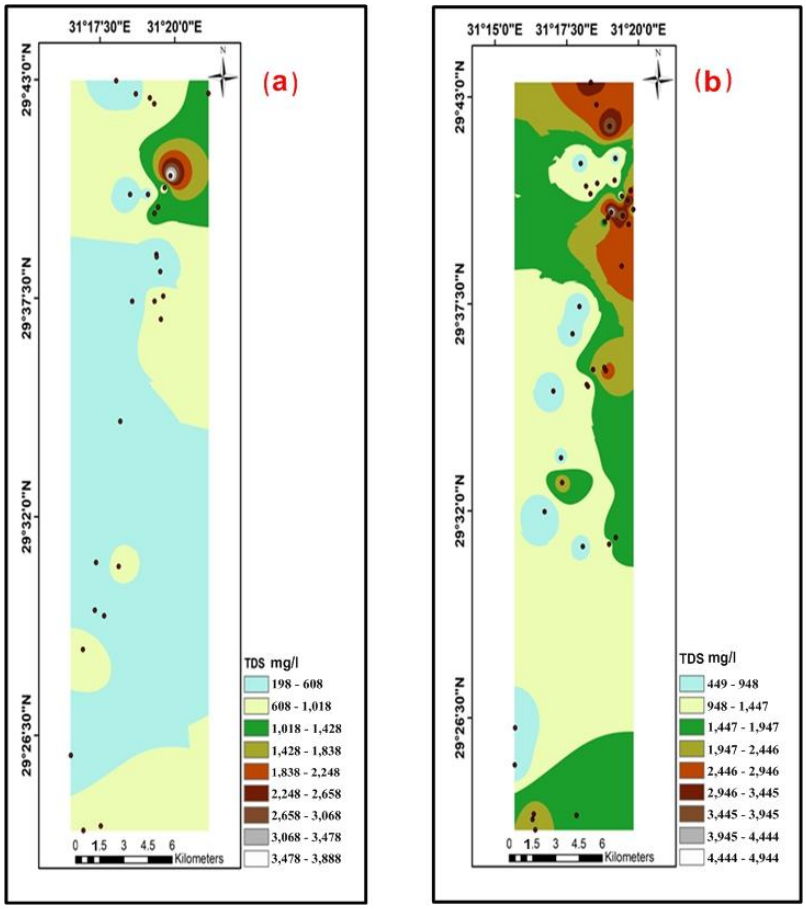

Fig. 15: Salinity zonation contour map of the Quaternary groundwater in a (Period, 2016) and b (Period, 2022) in the study area

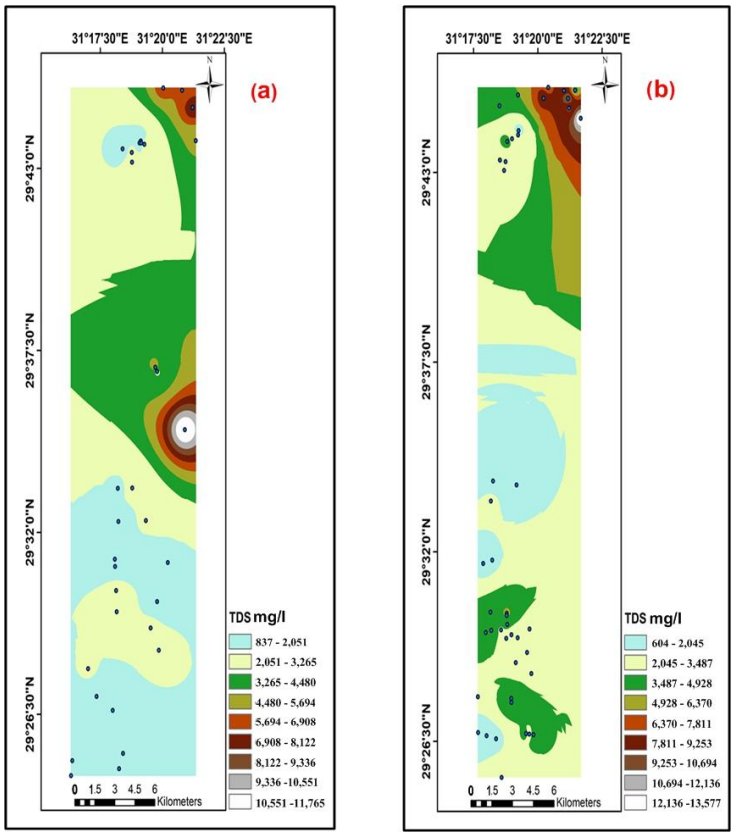

Fig.16: Salinity zonation contour map of the Pliocene groundwater in a (Period, 2016) and b (Period, 2022) in the study area

In the study area, the calcium content in the Quaternary groundwater samples varies between 12.18 and 316.8mg/l with an average value of 117.48mg/l, and between 16.67 and 366.66mg/l with an average value of 151.91mg/l during the periods 2016 and 2022, respectively (tables 3 & 4). Also, the calcium content in the Pliocene groundwater samples varies between 24.37 and 611.2mg/l with an average value of 198.53mg/l, and between 58.34 and 1541.66mg/l with an average value of 357.12mg/l during the periods 2016 and 2022, respectively (tables 3 & 4). The average values of calcium show an increasing trend to the east direction during the time from 2016 to 2022 for both the Quaternary and Pliocene aquifers as the salinity increases (Figs. 17a, 17b, 18a & 18b). It is noticed that, 58% and 88% of the Quaternary and Pliocene groundwater samples, respectively, in period 2016 (tables 3 & 4) have Ca^{2+} concentrations higher than the permissible limit 75mg/l (Egyptian Higher Committee for Water, 2007), while, 75% and 96% of the Quaternary and Pliocene groundwater samples in period 2022 (tables 3 & 4) have Ca^{2+} concentrations higher than the permissible limit.

Calcium may be significantly beneficial to human health when in acceptable concentrations in water. It is able to block the absorption of heavy metals in the human body, increase bone mass, and also prevent certain types of cancer (Bohlke, 2002). But in high concentrations, calcium may adversely affect human health by negatively affecting the absorption of other essential minerals in the body. Also, calcium (Ca^{2+}) occurs in most of the common rocks as a significant constituent, which is an essential elemental requirement for the growth of plants and animals (Jeong, 2001). The increase of Ca^{2+} concentrations may be related to the dissolution of carbonate rock formations (Pliocene rock formation), e.g., limestone, and potentially due to biodegradation or organic matter in upper soil horizons (Barzegar *et al.,* 2017). Also, the increase of Ca^{2+} concentration may be due to cation exchange processes (Deutsch and Siegel, 1997). Moreover, the high Ca^{2+} concentrations may also be related to anthropogenic activities (Wei *et al.,* 2022) and or due to industrial and municipal effluents (Anderson *et al.,* 2002), as well as the increase of calcium content in groundwater may come from the mixing processes of groundwater with wastewater of El Saff canal which seeps into the groundwater through faults and clastics (Fig. 7).

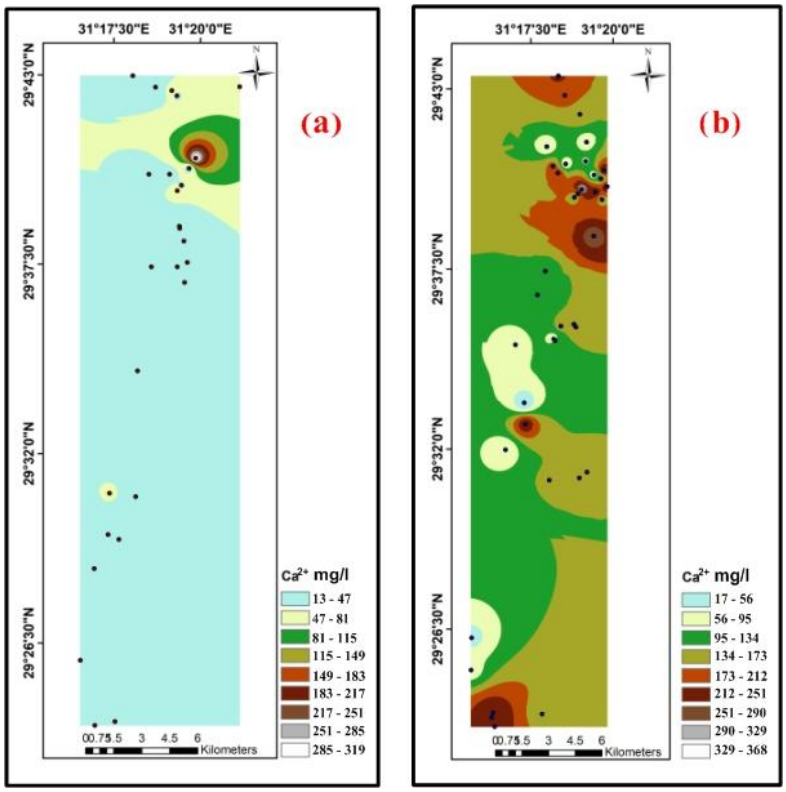

Fig. 17: Calcium zonation contour map of the Quaternary groundwater in a (period, 2016) and b (period, 2022) in the study area

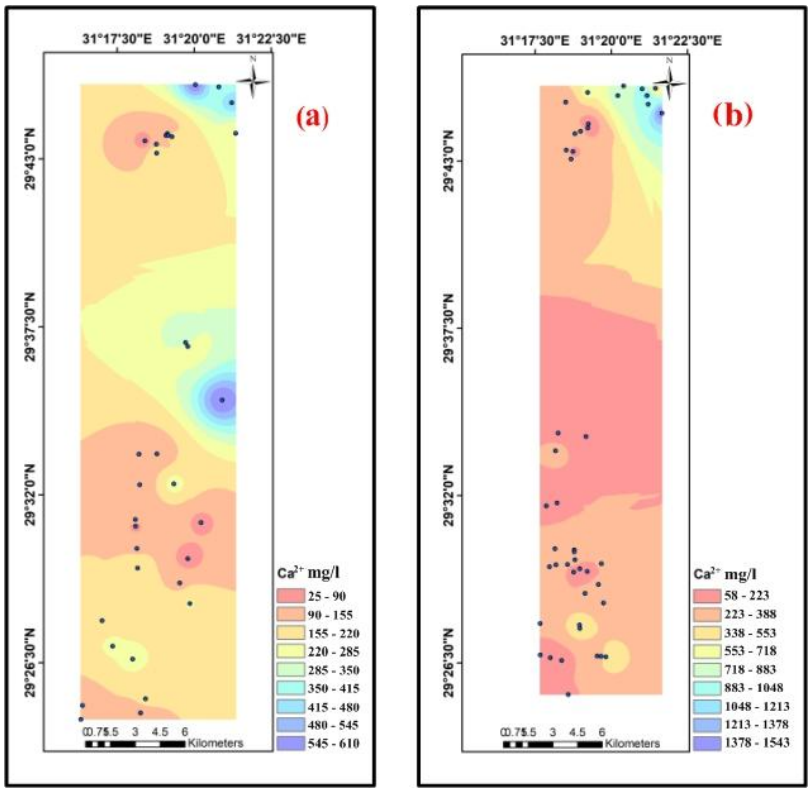

Fig. 18: Calcium zonation contour map of the Pliocene groundwater in a (period, 2016) and b (period, 2022) in the study area

In the study area, the sodium content in the Quaternary groundwater samples varies between 27 and 1105mg/l with an average value of 410mg/l, and between 36.78 and 1407mg/l with an average value of 431.45mg/l during the periods 2016 and 2022, respectively (tables 3 & 4) and (Figs. 19a & 19b). Also, the sodium content in the Pliocene groundwater samples varies between 191 and 3166mg/l with an average value of 755.88mg/l, and between 107 and 3146mg/l with an average value of 874.42mg/l during the periods 2016 and 2022, respectively (tables 3 & 4) and (Figs. 20a & 20b). The average values of sodium show a slightly increasing trend to the east as the salinity increases by time from 2016 to 2022 for both the Quaternary and Pliocene aquifers. This may be due to the dissolution of sodium-rich minerals such as clay and gravel, the return flow after irrigation water, municipal and/or industrial wastewater, landfill leachates, and anthropogenic activities. It is worth mentioning that excessive dietary sodium intake is associated with chronic diseases including hypertension, cardiovascular diseases, and kidney diseases (Zhang *et al.,* 2021).

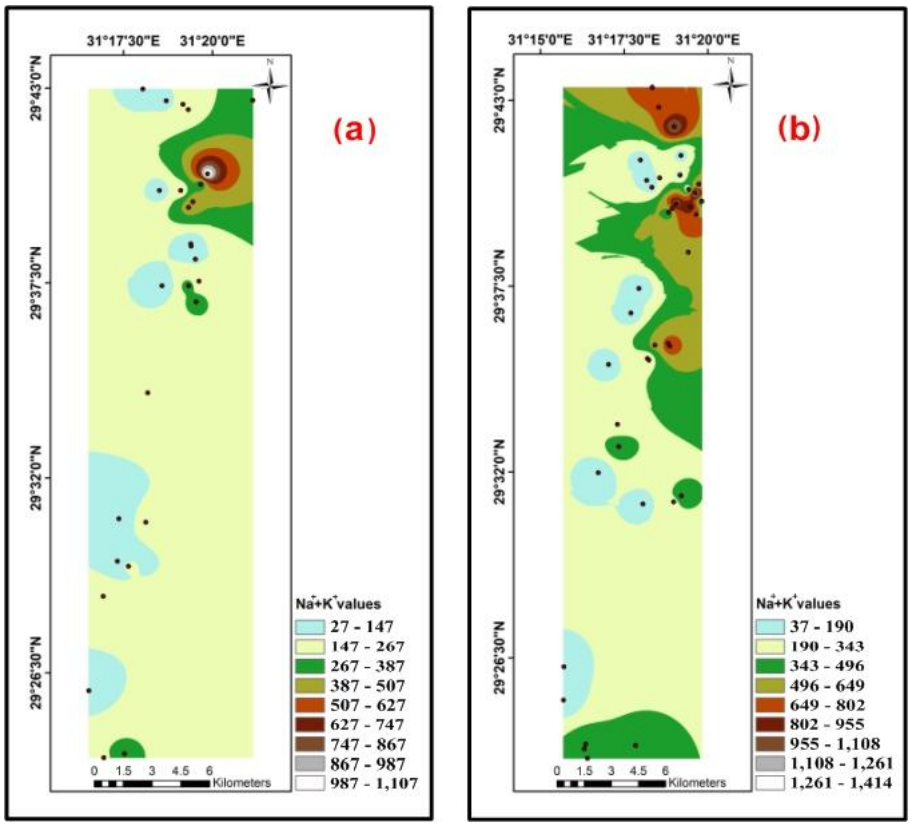

Fig. 19: Sodium zonation contour map of the Quaternary groundwater in a (period, 2016) and b (period, 2022) in the study area

In the study area, the bicarbonate concentration in the Quaternary groundwater samples varies between 97 and 455.5mg/l with an average value of 234.81mg/l, and between 77.13 and 412.28mg/l with an average value of 196.67mg/l during the periods 2016 and 2022, respectively (tables 3 & 4) and (Figs. 21a & 21b). Also, the bicarbonate concentration in the Pliocene groundwater samples varies between 85.33 and 414.46mg/l with an average value of 230.54mg/l, and between 58.06 and 343.62mg/l with an average value of 161.16mg/l during the periods 2016 and 2022, respectively (tables 3 & 4) and (Figs. 22a & 22b). It is noticed that the average values of bicarbonate show a slightly decreasing trend by time from 2016 to 2022 for both the Quaternary and Pliocene aquifers. The content of HCO_3^- has no known adverse health effects. The high bicarbonate content in groundwater in the study area is mainly related to the recharge from the irrigation canals. Also, the bicarbonate content in groundwater may be due to the seepage from El Saff canal for wastewater, and this was manifested by Panno *et al.,* (2001), who stated that alternate sources for HCO_3^- are also from the release of effluents from wastewater treatment plants, industrial and domestic sewage, cleaning agents, and food residues.

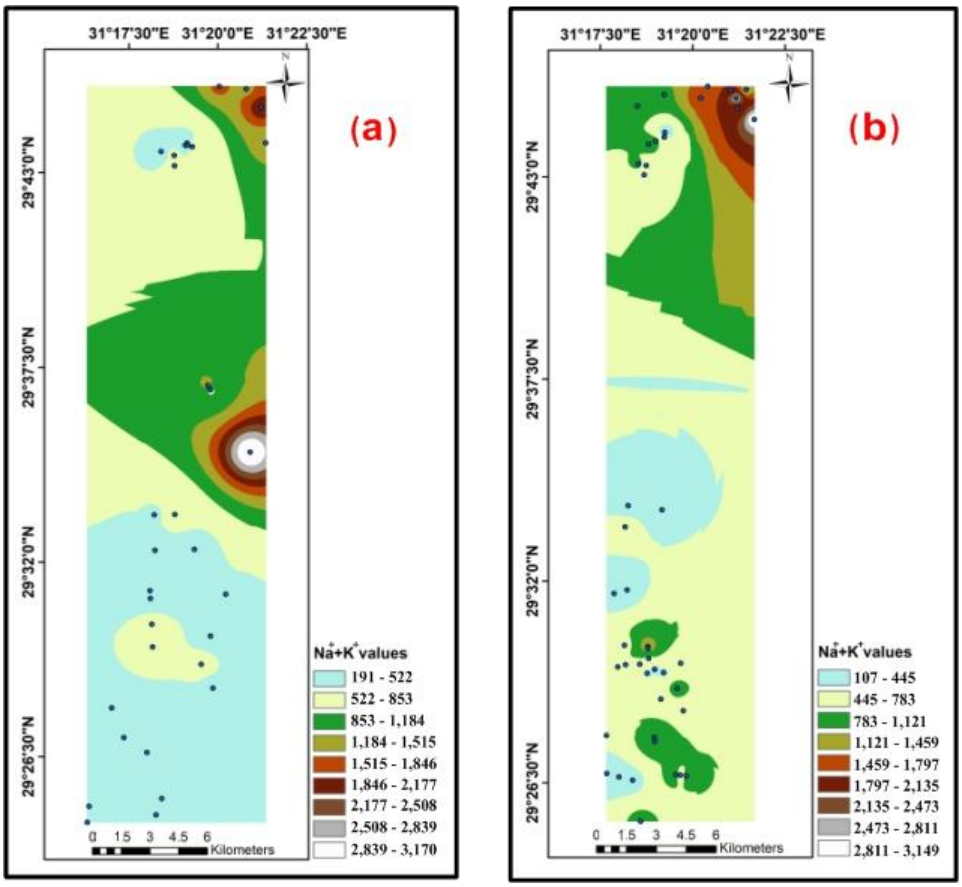

Fig. 20: Sodium zonation contour map of the Pliocene groundwater in a (period, 2016) and b (period, 2022) in the study area

Sulfate concentrations greater than 50mg/l cause a bitter taste in water, and higher concentrations of 400mg/l with calcium and magnesium can cause frailty in the body (Shankar *et al.,* 2008). In the study area, the sulfate concentration in the Quaternary groundwater samples varies between 15 and 950mg/l with an average value of 303.15mg/l, and between 55.7 and 1479.2mg/l with an average value of 555.94mg/l during the periods 2016 and 2022, respectively (tables 3 & 4) and (Figs. 23a & 23b). Also, the sulfate concentration in the Pliocene groundwater samples varies between 90 and 2942mg/l with an average value of 721.75mg/l, and between 43 and 2897.9mg/l with an average value of 1149.72mg/l during the periods 2016 and 2022, respectively (tables 3 & 4) and (Figs. 24a & 24b). It is noticed that the average values of sulfate show a slightly increasing trend by time from 2016 to 2022 for both the Quaternary and Pliocene aquifers, and the direction of increasing follows the same trend of salinity increase (Figs. 23a, 23b, 24a & 24b). This may be due to the dissolution of the gypsum mineral $CaSO_4.2H_2O$ included in the water-bearing strata and to the leaching of salts from soil close to the sulfate-rich desert zone. Also, the increase of sulfate concentration may be due to the anthropogenic activities such as seepage from El Saff canal for wastewater into both the Quaternary and Pliocene groundwater through faults and clastics (Fig. 7). Also, the concentration of sulfate may increase due to the return flow after irrigation and the excessive use of fertilizers.

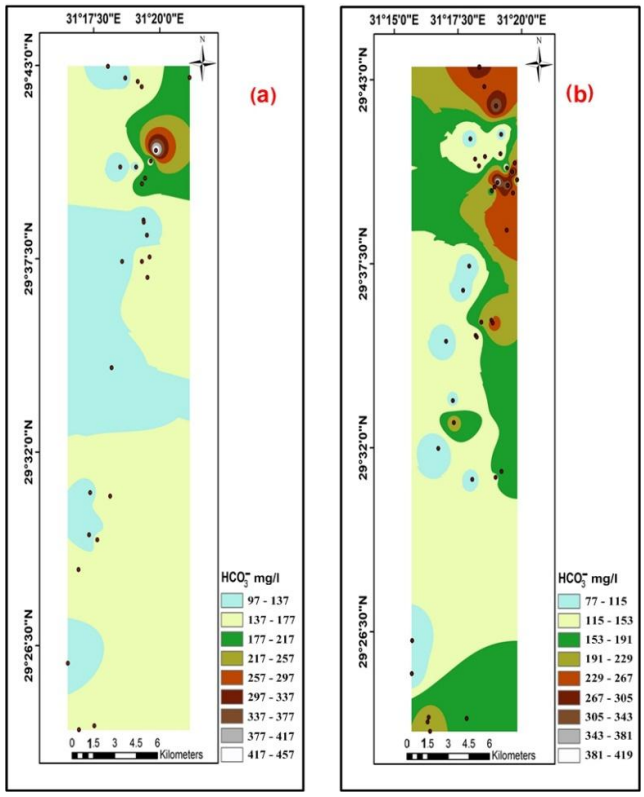

Fig. 21: Bicarbonate zonation contour map of the Quaternary groundwater in a (period, 2016) and b (period, 2022) in the study area

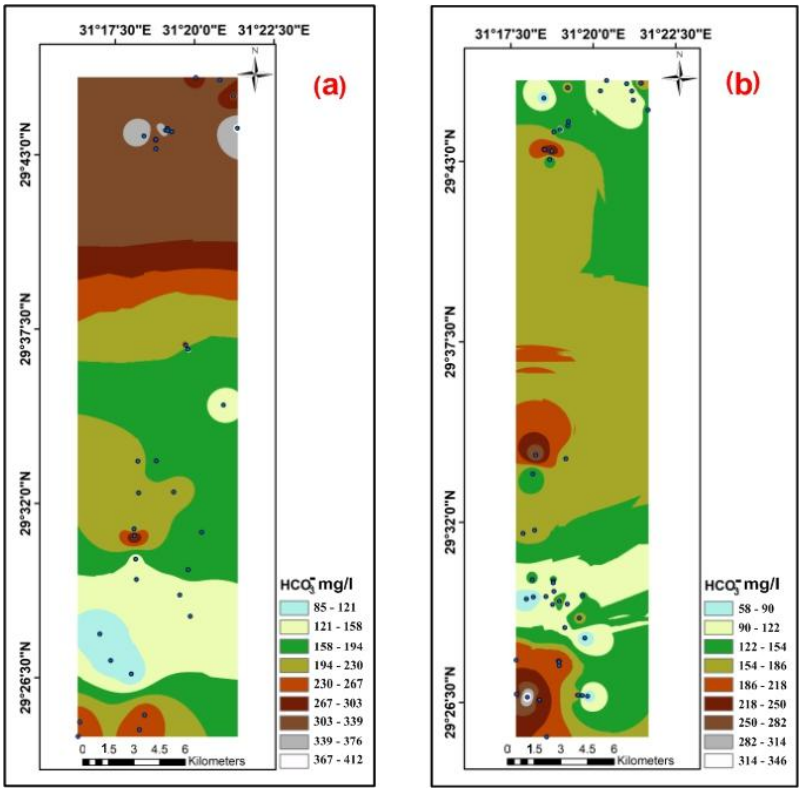

Fig. 22: Bicarbonate zonation contour map of the Pliocene groundwater in a (period, 2016) and b (period, 2022) in the study area

High chloride concentrations may impart an undesirable taste to potable water and could be very corrosive. Also, the high Cl^- concentration could be injurious to people suffering from heart and kidney diseases, and it can adversely affect soil porosity and permeability (Anim-Gyampo *et al.,* 2018). In the study area, the chloride concentration in the Quaternary groundwater samples varies between 19.72 and 1577.3mg/l with an average value of 539.58mg/l, and between 61.24 and 1974.1mg/l with an average value of 541.37mg/l during the periods 2016 and 2022, respectively (tables 3 & 4) and (Figs. 25a & 25b). Also, the chloride concentration in the Pliocene groundwater samples varies between 133 and 4654.3mg/l with an average value of 978.87mg/l, and between 111.35 and 5901.44mg/l with an average value of 1292.30mg/l during the periods 2016 and 2022, respectively (tables 3 & 4) and (Figs. 26a & 26b). It is noticed that the average values of chloride show a slightly increasing trend by time from 2016 to 2022 for both the Quaternary and Pliocene aquifers, and the direction of the increase follows the same trend of salinity increase (Figs. 25a, 25b, 26a & 26b). In addition, the higher chloride concentrations may be due to the halite dissolution, anthropogenic factors (e.g., sewage disposal, contamination from municipal and urban waste), and irrigation water return flow. This confirms the seepage from El Saff canal for wastewater to the groundwater in the study area through faults and clastics (Fig. 7).

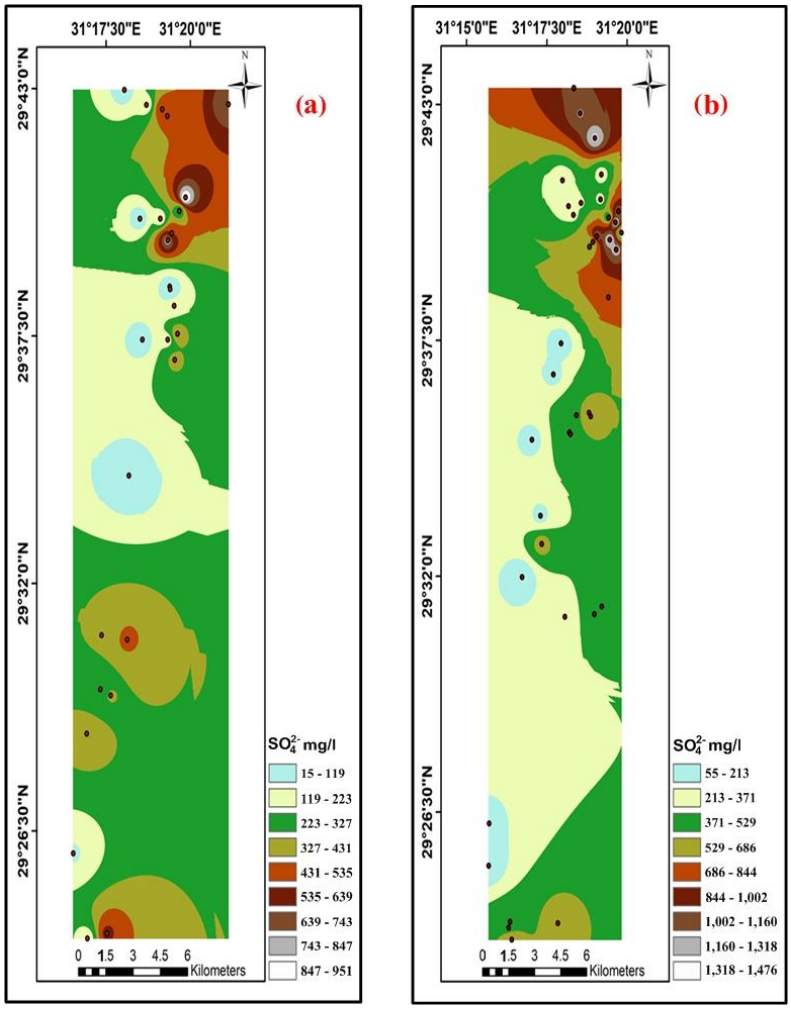

Fig. 23: Sulfate zonation contour map of the Quaternary groundwater in a (period, 2016) and b (period, 2022) in the study area

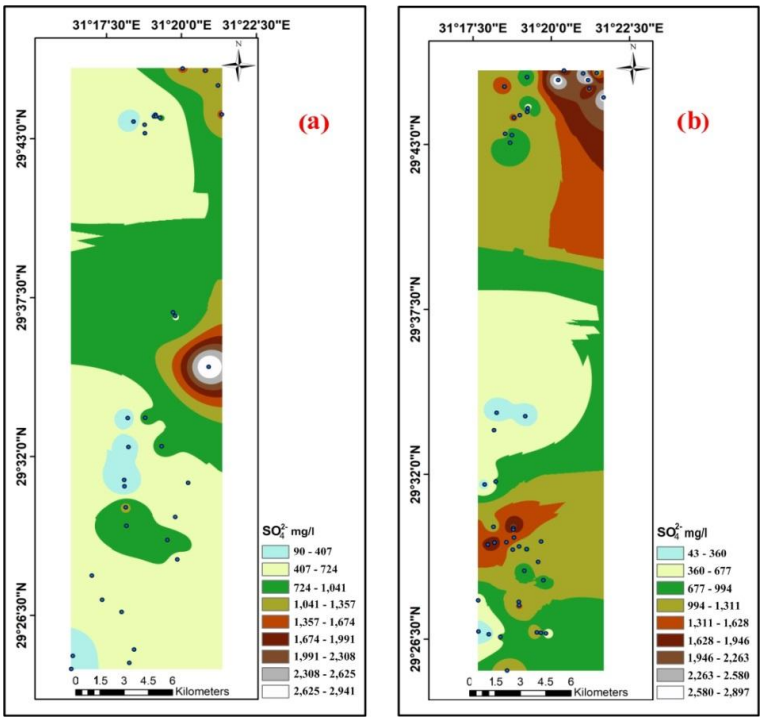

Fig. 24: Sulfate zonation contour map of the Pliocene groundwater in a (period, 2016) and b (period, 2022) in the study area

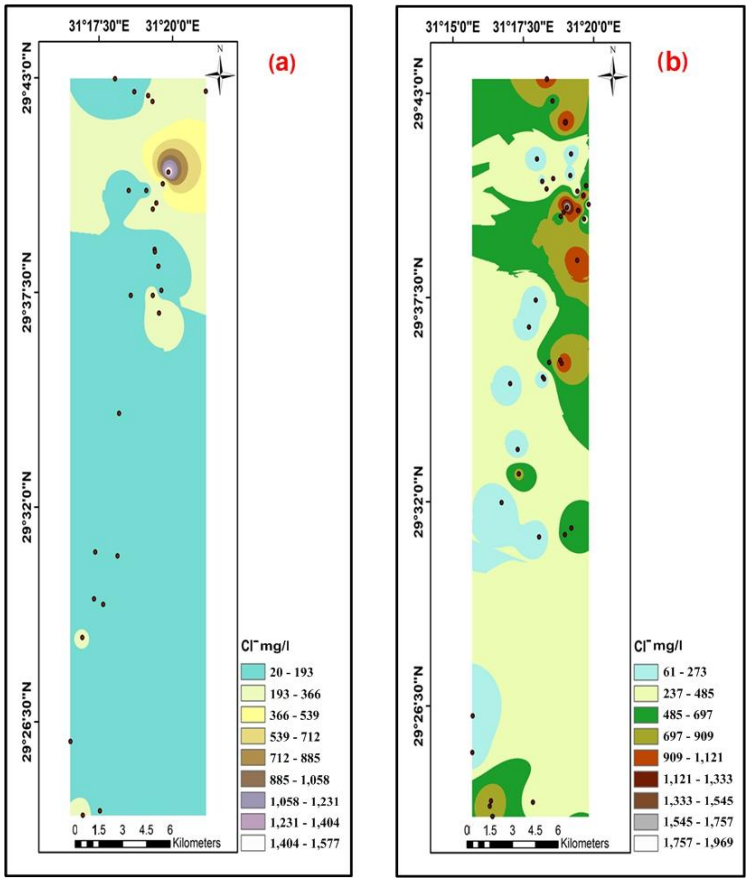

Fig.25: Chloride zonation contour map of the Quaternary groundwater in a (period, 2016) and b (period, 2022) in the study area

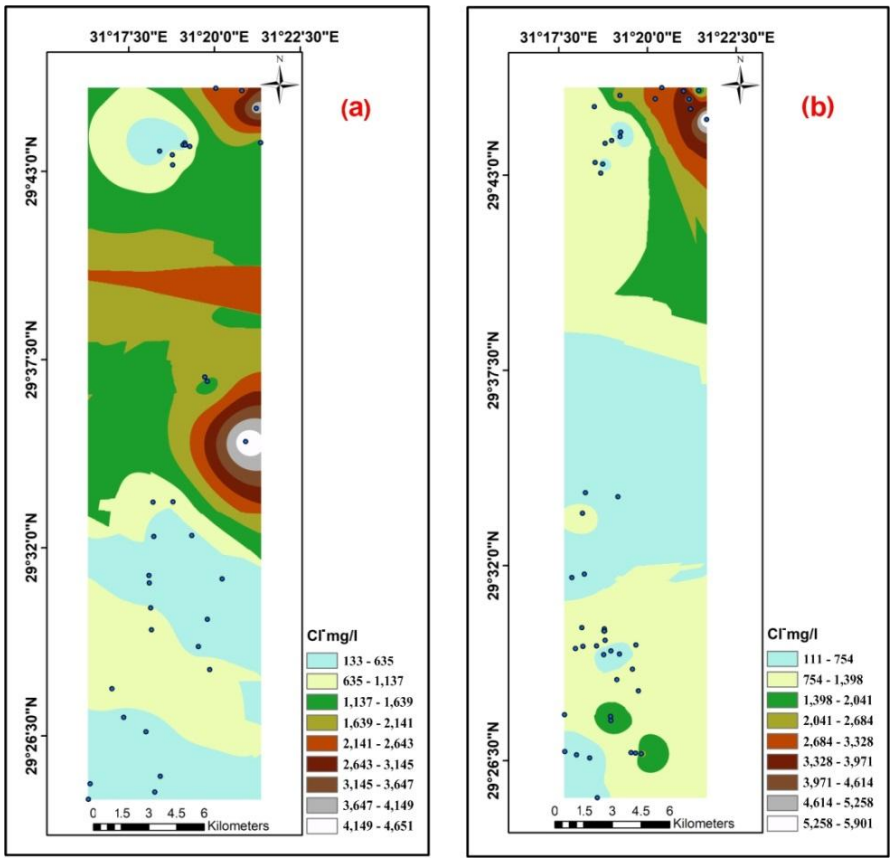

Fig. 26: Chloride zonation contour map of the Pliocene groundwater in a (period, 2016) and b (period, 2022) in the study area

In conclusion, during the process of groundwater flow, the chemical characteristics of groundwater are mainly affected by two types of factors: natural and anthropogenic activities. First, natural factors mainly refer to the formation lithology, geological structures, and recharge conditions in the flow area. Secondly, the anthropogenic activities factor mainly refers to the agricultural activity, industrial water and wastewater discharge, as well as groundwater exploitation.

Table 3: The electrical conductivity (µS/cm) at 25^0C, pH, salinity, and major cations and anions concentrations in the Quaternary and Pliocene groundwater samples as mg/l (period, 2016)

Statistics	Parameters								
	EC	pH	TDS	Ca^{2+}	Mg^{2+}	$Na^{+}+K^{+}$	$CO_3^{2-}+HCO_3^{-}$	SO_4^{2-}	Cl^{-}
Quaternary groundwater samples									
Minimum	349	7.02	198	12.18	3.87	27	97	15	19.72
Maximum	6390	8.32	3856	316.8	108.55	1105	455.5	950	1577.3
Average	2707	7.82	1587.52	117.48	46.34	410.02	234.81	303.15	541.37
Pliocene groundwater samples									
Minimum	1565	7.11	836	24.37	6.1	191	85.33	90	133
Maximum	18384	8.08	11766	611.2	307.2	3166	414.46	2942	4654.3
Average	4583.27	7.71	2800.48	198.53	76.79	755.88	230.54	721.75	978.87

Table 4: The electrical conductivity (µS/cm) at 25^0C, pH, salinity, and major cations and anions concentrations in Quaternary and Pliocene groundwater samples as mg/l (period, 2022)

Statistics	Parameters								
	EC	pH	TDS	Ca^{2+}	Mg^{2+}	$Na^{+}+K^{+}$	$CO_3^{2-}+HCO_3^{-}$	SO_4^{2-}	Cl^{-}
Quaternary groundwater samples									
Minimum	850	7.16	449	16.67	20.25	36.78	77.13	55.7	61.24
Maximum	8370	8.9	4954	366.66	151.87	1407	412.28	1479.2	1974.1
Average	3002.68	7.83	1850.45	151.91	61.13	431.45	196.67	555.94	593.58
Pliocene groundwater samples									
Minimum	1260	7.03	603	58.34	22.78	107	58.06	43	111.35
Maximum	20000	8.64	13578	1541.7	394.87	3146	343.62	2897.9	5901.4
Average	6122.39	7.79	3820.43	357.12	103.25	874.42	161.16	1149.7	1292.3

A Piper diagram can help to understand the potential hydrochemical processes controlling groundwater chemistry (Perera *et al.,* 2022). The hydrochemical data of surface water samples (irrigation canals and El Saff canal for wastewater) and groundwater samples (Quaternary and Pliocene aquifers) in the study area were plotted on a Piper triangular diagram (Piper, 1944), (Figs. 27 & 28).

The results showed differences in the distribution of the sampling points between the period (2016) and the period (2022). Whereas, the majority of the groundwater samples (61% of the Quaternary groundwater samples and 82% of the Pliocene groundwater samples) and surface water samples (50% of El Saff canal for wastewater samples and 38% of the irrigation canals water samples) in the study area in period (2016) lie in sub-area (7). Also, the majority of the groundwater samples (58% of the Quaternary groundwater samples and 74% of the Pliocene groundwater samples) and surface water samples (56% of El Saff canal for wastewater samples and 13% of the irrigation canals water samples) in the study area in period (2022) lie in sub-area (7), indicating that the Quaternary groundwater is influenced by the Pliocene groundwater due to upward leakage through faults and clastics (Fig. 7) as the two aquifers are hydraulically connected as well as both the Quaternary and Pliocene groundwater samples are recharged from the irrigation canals and El Saff canal for wastewater through seepage.

While 18% and 15% of the Quaternary and Pliocene groundwater samples as well as 33% of El Saff canal for wastewater samples in the study area in period (2016) lie in sub-area (9). Also, 33% and 17% of the Quaternary and Pliocene groundwater samples, respectively, as well as 50% of the irrigation canals water samples and 22% of El Saff canal for wastewater samples in the study area in period (2022) lie in sub-area (9), indicating that the Quaternary and Pliocene groundwater samples are influenced by direct recharge from El Saff canal for wastewater.

Noteworthy mention that, 18% of the Quaternary groundwater samples and 50% of the irrigation canals water samples, as well as 17% of El Saff canal for wastewater samples in the study area in period (2016) lie in sub-area (5). Also, 5% of the Quaternary groundwater samples and 38% of the irrigation canals water samples in the study area in period (2022) lie in sub-area (5), indicating that the Quaternary groundwater samples in the old lands are recharged from the irrigation canal and El Saff canal for wastewater.

Finally, one groundwater sample tapping for both the Quaternary and Pliocene aquifers, respectively, in the study area in period (2016) lies in sub-area (6). Also, 4% and 9% of the Quaternary and Pliocene groundwater samples, respectively, as well as 22% of El Saff canal for wastewater samples, in the study area in period (2022) are lying in sub-area (6), indicating that the groundwater of the two aquifers is affected by leaching and dissolution processes and is also affected by El Saff canal for wastewater by seepage.

From the above mentioned discussions, it is obvious that both the Quaternary and Pliocene groundwater deteriorated by time from 2016 to 2022, as the percentage of the groundwater samples affected by El Saff canal for wastewater increased by time from 2016 to 2022.

Geochemical modeling

The inverse geochemical model NETPATH was used to interpret the geochemical processes of water along real or hypothetical flow paths in aquifers or other hydrologic systems using hydrochemical data.

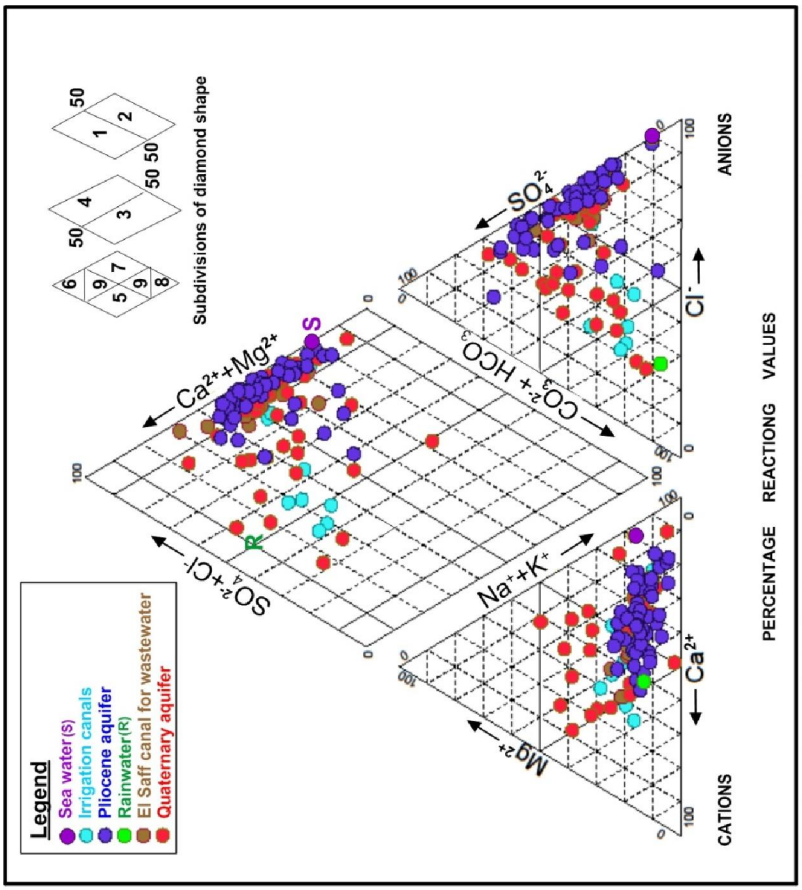

Fig.27 Piper diagram for the Quaternary and Pliocene groundwater (Period, 2016) at the study area

Fig.28 Piper diagram for the Quaternary and Pliocene groundwater (Period, 2022) at the study area

Notes; 1.Alkaline earths exceeding alkalies, 2.Alkalies exceeding alkaline earths, 3.Weak acids exceeding strong acids, 4.Strong acids exceeding weak acids, 5.Carbonate hardness exceeds 50%, 6.Non-carbonate hardness exceeds 50%, 7.Alkalies and strong acids predominated, 8.Alkaline earths and weak acids predominated, 9.Mixed type

Also, it was used to compute the mixing proportions of different water resources according to changes of chemical composition in groundwater along a flow path or the effect of surface water recharge.

The NETPATH model results showed that both the Quaternary and Pliocene groundwater samples in the study area in periods 2016 and 2022 were affected by the mixing with both El Saff canal for wastewater and the irrigation canals (initial waters) through the infiltration and dissolution processes of the aquifer matrix.

It was noticed that the mixing of the wastewater of El Saff canal with the Quaternary and Pliocene groundwater samples in the study area increased by time from 2016 to 2022, where the maximum mixing ratios ranged from 65% to 66% for the Quaternary aquifer (table 5) and from 72% to 96% for the Pliocene aquifer (table 6). On the other hand, the geochemical processes of the Quaternary and Pliocene groundwater samples in the study area increased by time from 2016 to 2022, where the maximum values ratios ranged from 60% to 78% for the Quaternary aquifer (table 5) and from 43% to 45% for the Pliocene aquifer (table 6).

Table 5: NETPATH reaction and mixing model results for selected groundwater samples tapping the Quaternary aquifer in periods 2016 and 2022

Model Type	Initial Water				Final water	Mixing Ratio (%)			
	Initial No.1	Initial No.2	Initial No.3	Initial No.4					
Reaction model	Irrigation canal water	Wastewater of El Saff canal at north of the atudy area	Wastewater of El Saff canal at south of the atudy area	Quaternary aquifer		1	2	3	4
				Period, 2016					
Mixing Model	Sample No.3	Sample No.16	Sample No.20	Quaternary groundwater sample	Sample No.28	1%	32%	7%	60%
					Sample No.29	24%	21%	44%	11%
					Sample No.37	45%	5%	33%	17%
					Sample No.42	65%	5%	20%	10%
					Sample No.47	39%	18%	27%	16%
				Period, 2022					
Mixing Model	Sample No.5	Sample No.10	Sample No.16	Quaternary groundwater sample	Sample No.28	19%	0%	62%	19%
					Sample No.36	31%	20%	13%	36%
					Sample No.38	0%	1%	21%	78%
					Sample No.45	24%	11%	53%	12%
					Sample No.46	0%	27%	39%	34%

Water pollution

The pollution of the surface water and groundwater in the study area can be discussed by detecting and studying some minor constituents' concentrations, such as nitrate and boron, as well as some trace elements concentrations, such as aluminum, iron, manganese and lead in the concerned surface water and groundwater in the investigated area. Where, if the concentrations of those minor constituents and/or trace elements in the surface water and groundwater in the study area increased greater than the acceptable limits according to WHO (2017), the concerned water would become polluted and thus deteriorated.

Table 6: NETPATH reaction and mixing model results for selected groundwater samples tapping the Pliocene aquifer in periods 2016 and 2022

Model Type	Initial Water				Final water	Mixing Ratio (%)			
	Initial No.1	Initial No.2	Initial No.3	Initial No.4					
Reaction model	Irrigation canal water	Wastewater of El Saff canal at north of the atudy area	Wastewater of El Saff canal at south of the atudy area	Pliocene aquifer water		1	2	3	4
Period, 2016									
Mixing Model	Sample No.3	Sample No.16	Sample No.20	Pliocene groundwater sample	Sample No.63	32%	61%	0%	7%
					Sample No.69	10%	47%	0%	43%
					Sample No.77	14%	43%	22%	21%
					Sample No.79	40%	57%	0%	3%
					Sample No.81	28%	72%	0%	0%
Period, 2022									
Mixing Model	Sample No.5	Sample No.10	Sample No.16	Pliocene groundwater sample	Sample No.61	0%	59%	18%	23%
					Sample No.70	0%	44%	52%	4%
					Sample No.84	8%	23%	50%	19%
					Sample No.94	29%	0%	26%	45%

Surface water pollution

It is obvious that the irrigation canals (El Hager, El Khashab and Masjid Musi alqabliya canals) in the study area in periods 2016 and 2022 have a slight increase of Al, Cr, Cu, Ni and Zn concentrations (tables 7 and 8). whereas, in period (2016), these irrigation canals have nitrate, boron, iron, manganese and lead concentrations ranging from 0.1 to 34.399mg/l with an average value of 14.38mg/l, from 0.0281 to 1.107mg/l with an average value of a 0.26mg/l, from 0.449 to 3.097mg/l with an average value of 1.74mg/l, from 0.0659 to 0.6183mg/l with an average value of 0.238mg/l and from 0.0477 to 0.1224mg/l with an average value of 0.072mg/l, respectively (table 7). While, in period 2022, these canals have nitrate, boron, iron, manganese and lead concentrations ranging from 8.9 to 48.3mg/l with an average value of 25.25mg/l, from 0.138 to 9.55mg/l with an average value of a 3.999mg/l, from 0.166 to 24.54mg/l with an average value of 7.579mg/l, from 0.014 to 1.64mg/l with an average value of 0.4284mg/l and from 0.0495 to 0.168mg/l with an average value of 0.074mg/l, respectively (table 8). It was noticed that the concentrations of nitrate, boron, iron, manganese and lead in the irrigation canals increased by time from 2016 to 2022, and this can be attributed to the following:

1-The effect of spreading solid and liquid industrial wastes that produced from some small factories built on the sides of the irrigation canals which are currently discharged into El Khashab and El Hager canals as well as the River Nile, and certainly pollutes such water.

2- These irrigation canals act as drains for different human activities as municipal wastewater in some localities in the study area.

3- The drain of the wastewater of El Saff canal (which contains varying pollutants) into the River Nile as at El Ghammazah area (Fig. 14a), which in turn moves again to the irrigation canals. Whereas, El Saff canal for wastewater at the study area in period (2016) has nitrate, boron, iron, manganese and lead concentrations ranging from 0.1 to 87.613mg/l with an average value of 28.78, from 0.2876 to 1.185mg/l with an average value of 0.689mg/l, from 0.305 to 6.707mg/l with an average value of 2.98mg/l, from 0.01 to 0.2539mg/l with an average value of 0.1213mg/l and from 0.0515 to 0.31mg/l with an average value of 0.12mg/l, respectively (table 7). While, in period (2022), El Saff canal for wastewater has nitrate, boron, iron, manganese and lead concentrations ranging from 12.6 to 134.4mg/l with an average value of 61.8, from 0.0.113 to 16.84mg/l with an average value of 2.96mg/l, from 0.582

to 30.56mg/l with an average value of 9.27mg/l, from 0.066 to 1.47mg/l with an average value of 0.446mg/l and from 0.0036 to 0.188mg/l with an average value of 0.0513mg/l, respectively (table 8). This means that, the nitrate, boron, iron, manganese and lead concentrations in El Saff canal for wastewater increased by time from 2016 to 2022, which confirmed that the water of the irrigation canals deteriorated by time from 2016 to 2022.

Table 7: The concentrations of trace elements and minor constituents in the surface water samples as mg/l (Period, 2016)

Statistics	Parameters									
	Al	**Cr**	**Cu**	**Fe**	**Mn**	**Ni**	**Zn**	**Pb**	**B**	**NO_3^-**
Irrigation canals										
Minimum	0.06	0.007	0.004	0.449	0.0659	0.002	0.0193	0.0477	0.0281	0.1
Maximum	2.396	0.0092	0.0658	3.097	0.6183	0.046	0.1761	0.1224	1.107	34.399
Average	1.0754	0.0072	0.019	1.7434	0.2375	0.0107	0.0691	0.0717	0.2641	14.382
El Saff canal for wastewater										
Minimum	0.0103	0.0041	0.004	0.305	0.01	0.002	0.0257	0.0515	0.2876	0.1
Maximum	3.384	0.0322	0.1228	6.707	0.2539	0.0297	4.105	0.31	1.185	87.613
Average	0.5946	0.0086	0.0476	2.9822	0.1213	0.0103	0.6410	0.1191	0.6894	28.7785
Permissible limits (WHO, 2017)	0.2	0.05	2	0.3	0.4	0.07	5	0.01	0.5	50

Table 8: The concentrations of trace elements and minor constituents in the surface water samples as mg/l (Period, 2022)

Statistics	Parameters									
	Al	**Cr**	**Cu**	**Fe**	**Mn**	**Ni**	**Zn**	**Pb**	**B**	**NO_3^-**
Irrigation canals										
Minimum	0.097	0.002	0.005	0.166	0.014	0.0001	0.009	0.0495	0.138	8.9
Maximum	2.99	0.004	0.016	24.54	1.64	0.017	0.463	0.168	9.55	48.3
Average	1.0953	0.0029	0.0045	7.579	0.4284	0.0045	0.1938	0.0738	3.9994	25.25
El Saff canal for wastewater										
Minimum	0.056	0.003	0.001	0.582	0.066	0.0003	0.005	0.0036	0.113	12.6
Maximum	4.08	0.011	0.911	30.56	1.47	0.014	0.456	0.188	16.84	134.4
Average	0.7828	0.004	0.1039	9.2713	0.4464	0.0046	0.2084	0.0513	2.9617	61.8

Groundwater Pollution

Nitrate (NO_3^-) is considered as a primary contributor to groundwater pollution due to its stability, high solubility and mobility. Drinking water containing high levels of nitrate has been associated with the risk of methemoglobinemia or 'blue baby syndrome' (Fan and Steinberg, 1996), and cancer through the formation of carcinogenic N-nitroso compounds (Weyer *et al.,* 2001).

In the study area, the nitrate concentration in the Quaternary groundwater samples varies between 0.377 and 79.87mg/l with an average value of 34.93mg/l, and between 2.1 and 194mg/l with an average value of 55.49mg/l during the periods 2016 and 2022, respectively (tables 9 & 10) and (Figs. 29a & 29b). Also, the nitrate concentration in the Pliocene groundwater samples varies between 17.033 and 81.992mg/l with an average value of 48.194mg/l, and between 10.5 and 241.1mg/l with an average value of 102.675mg/l during the periods 2016 and 2022, respectively (tables 9 & 10) and (Figs. 30a & 30b). It is obvious that 21% and 48% of the Quaternary and Pliocene groundwater samples, respectively, in period (2016) have nitrate concentrations more than 50mg/l violating the drinking water limits (WHO, 2017), while 48% and 52% of the Quaternary and Pliocene groundwater samples, respectively,

in period (2022) have nitrate concentrations more than 50mg/l. This means that the nitrate concentration in the groundwater samples in the study area increased by time from period (2016) to period (2022).

It is clear that the direction of increasing of the nitrate concentrations in the Quaternary groundwater samples in the two periods (2016 and 2022) is from south to north of the study area (Figs. 29a and 29b). Whereas the direction of increasing of the nitrate concentration in the Pliocene groundwater samples in the period (2016) is from both the northeastern and southwestern portions to the middle of the study area (Fig. 30a), while in period (2022) the direction of increasing is to the northeastern and southeastern portions of the study area (all over the area), (Fig. 30b).

It is noticed that the average values of nitrate concentrations (tables 9 & 10) show a valuable increasing trend during time from 2016 to 2022 for the Quaternary and Pliocene groundwater samples. These high nitrate concentrations are mainly attributed to intense fertilization and irrigation water return flow, groundwater over pumping and the released wastewater. This confirms the seepage from El Saff canal for wastewater to the groundwater in the study area through faults and clastics (Fig.7). This means that the effect of El Saff canal for wastewater on the groundwater in the study area increased by time from 2016 to 2022. Consequently, the concerned groundwater in the study area became more polluted, and this led to its deterioration by time. This is manifested by Gu *et al.,* (2012) who stated that the increased levels of (NO_3^-) in groundwater are primarily caused by anthropogenic activities such as the overuse of nitrogen fertilizers and animal manures, the discharge of domestic and industrial sewage, and the high atmospheric N deposition.

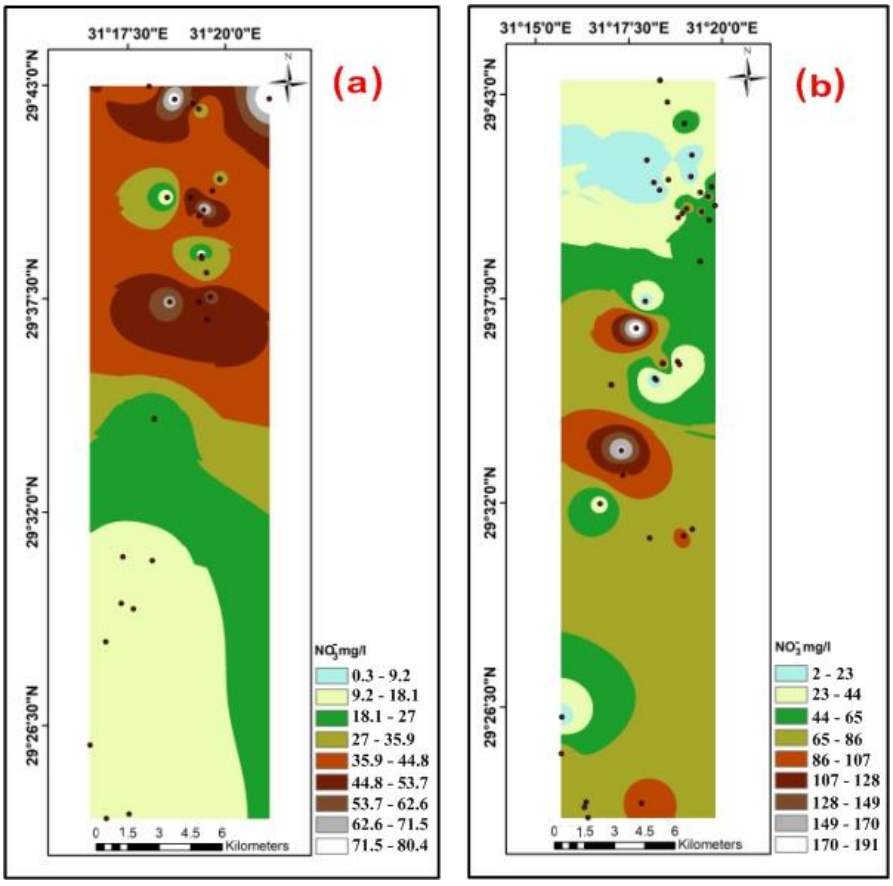

Fig.29: Nitrate zonation contour map of the Quaternary groundwater in a (Period, 2016) and b (Period, 2022) in the study area

The occurrence of boron in groundwater is necessary due to its considerable impact on human physiology. In the study area, the boron concentration in the Quaternary groundwater samples varies between 0.0151 and 2.683mg/l with an average value of 0.67mg/l, and between 0.052 and 16.83mg/l with an average value of 3.22mg/l during the periods 2016 and 2022, respectively (tables 9 & 10) and

(Figs. 31a & 31b). Also, the boron concentration in the Pliocene groundwater samples varies between 0.0151 and 2.359mg/l with an average value of 0.547mg/l, and between 0.003 and 17.15mg/l with an average value of 6.45mg/l during the periods 2016 and 2022, respectively (tables 9 & 10) and (Figs. 32a & 32b). It is obvious that 48% and 37% of the Quaternary and Pliocene groundwater samples, respectively, in period (2016) have boron concentrations more than 0.5mg/l violating the drinking water limits (WHO, 2017), while 52% and 84% of the Quaternary and Pliocene groundwater samples, respectively, in period (2022) have boron concentrations more than 0.5mg/l. This means that the boron concentration in the groundwater samples in the study area increased by time from period (2016) to period (2022).

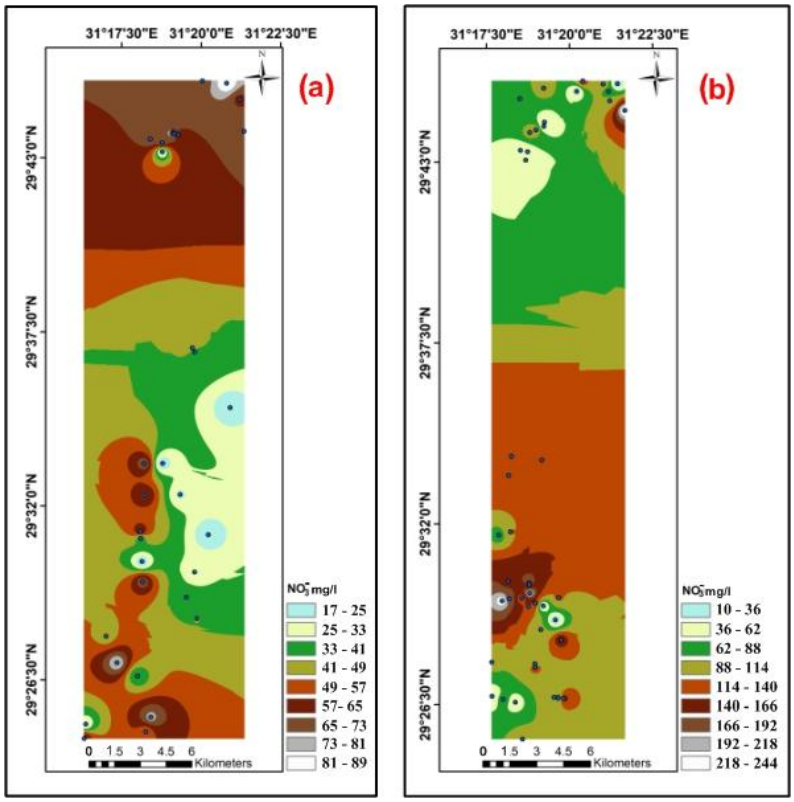

Fig. 30: Nitrate zonation contour map of the Pliocene groundwater in a (Period, 2016) and b (Period, 2022) in the study area

It is clear that the direction of increase of the boron concentrations in the Quaternary and Pliocene groundwater samples in period (2016) is to the north of the study area (Figs. 31a and 32a), while in period (2022) the boron concentrations in the Quaternary and Pliocene groundwater samples increase all over the study area (Figs. 31b and 32b).

It is noticed that the average values of boron concentrations show a valuable increasing trend by time from 2016 to 2022 for both the two Quaternary and Pliocene aquifers. These high concentrations could be attributed to contamination from the released wastewater (which contains domestic water that includes detergents that use borates in their manufacture) and irrigation water return flow. This confirms the seepage from El Saff canal for wastewater to the groundwater in the study area through faults and clastics (Fig. 7). This means that the effect of El Saff canal for wastewater on the groundwater in the study area increased by time from 2016 to 2022. Consequently, the concerned groundwater in the study area became more polluted and, in turn, deteriorated by time.

It is clear that some of the Quaternary and Pliocene groundwater samples in the study area in the two periods (2016 and 2022) contain slight concentrations of Al, Cr, Cu, Ni and Zn (tables 9 & 10), while the rest of the samples have valuable concentrations of Fe, Mn and Pb in the two periods (2016 and 2022).

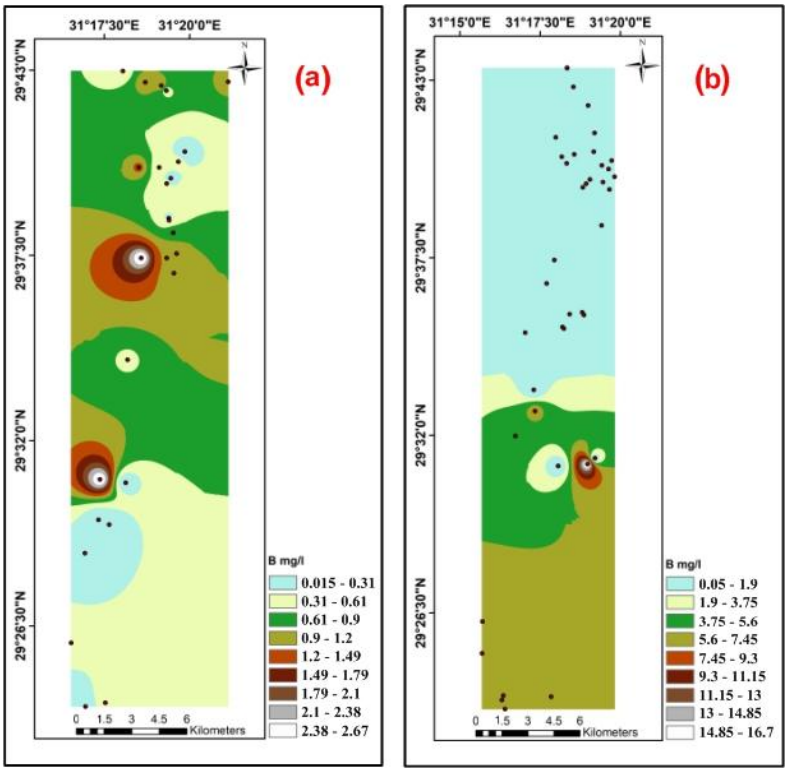

Fig. 31: Boron zonation contour map of the Quaternary groundwater in a (Period, 2016) and b (Period, 2022) in the study area

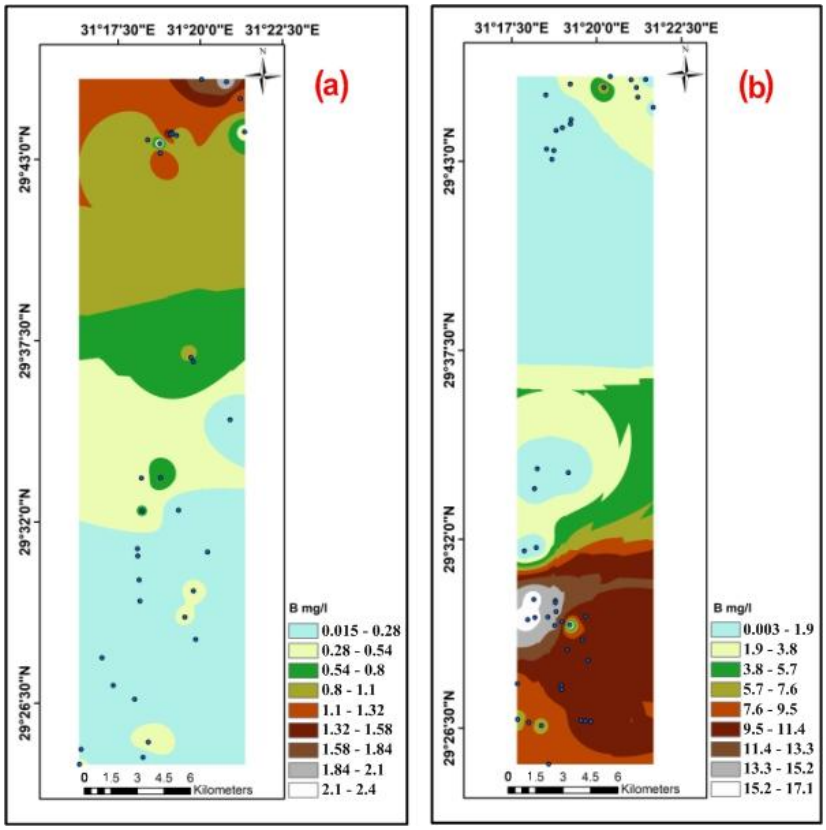

Fig. 32: Boron zonation contour map of the Pliocene groundwater in a (Period, 2016) and b (Period, 2022) in the study area

The iron concentration in the Quaternary groundwater samples varies between 0.0068 and 3.835mg/l with an average value of 0.5196mg/l, and between 0.009 and 11.53mg/l with an average value of 1.0031mg/l during the periods 2016 and 2022, respectively (tables 9 & 10) and (Figs. 33a & 33b). Also, the iron concentration in the Pliocene groundwater samples varies between 0.002 and 6.729mg/l with an average value of 1.049mg/l, and between 0.009 and 4.8mg/l with an average value of 0.492mg/l during the periods 2016 and 2022, respectively (tables 9 & 10) and (Figs. 34a & 34b). It is noticed that the average values of iron concentrations show a valuable increase by time from 2016 to 2022 for the Quaternary groundwater samples. On the contrary, the average values of iron concentrations show a slight decrease by time from 2016 to 2022 for the Pliocene groundwater samples. 41% and 69% of the Quaternary and Pliocene groundwater samples, respectively, in period (2016) have iron concentrations more than 0.3mg/l violating the drinking water limits (WHO, 2017), while 51% and 20% of the Quaternary and Pliocene groundwater samples, respectively, in period (2022) have iron concentrations more than 0.3mg/l. This means that the iron concentration in the Quaternary groundwater samples in the study area slightly increases by time from period (2016) to period (2022). It is worth mentioning that the high concentration of iron in the groundwater more than the permissible limit (0.3mg/l) leads to some problems for humans, such as kidney failure.

The manganese concentration in the Quaternary groundwater samples varies between 0.0004 and 0.524mg/l with an average value of 0.0778mg/l, and between 0.0004 and 0.793mg/l with an average value of 0.09827mg/l during the periods 2016 and 2022, respectively (tables 9 & 10). Also, the manganese concentration in the Pliocene groundwater samples varies between 0.0004 and 0.5156mg/l with an average value of 0.1227mg/l, and between 0.0003 and 2.62mg/l with an average value of 0.1377mg/l during the periods 2016 and 2022, respectively (tables 9 & 10). It is noticed that the average values of manganese concentrations show an increasing trend by time from 2016 to 2022 for both the two Quaternary and Pliocene groundwater samples. Also, it is obvious that 3% and 6% of the Quaternary and Pliocene groundwater samples, respectively, in period (2016) have manganese concentrations more than 0.4mg/l violating the drinking water limits (WHO, 2017), while 5% and 7% of the Quaternary and Pliocene groundwater samples, respectively, in period (2022) have manganese concentrations more than 0.4mg/l. This means that the manganese concentration in the groundwater samples in the study area increased by time from period (2016) to period (2022). The high levels of manganese in groundwater are concerning as it is a powerful neurotoxin that may lead to learning disabilities, deficits in intellectual function, compulsive behavior, and attention disorder in children (Wasserman *et al.,* 2006). While, in the elderly, the high levels of manganese may cause Parkinson's disease (WHO, 2021).

The lead concentration in the Quaternary groundwater samples varies between 0.0021 and 0.3011mg/l with an average value of 0.07118mg/l, and between 0.0011 and 0.099mg/l with an average value of 0.0074mg/l during the periods 2016 and 2022, respectively (tables 9 & 10) and (Figs. 35a & 35b). Also, the lead concentration in the Pliocene groundwater samples varies between 0.0013 and 0.1669mg/l with an average value of 0.04834mg/l, and between 0.0014 and 0.0198mg/l with an average value of 0.01033mg/l during the periods 2016 and 2022, respectively (tables 9 & 10) and (Figs. 36a & 36b). It has been noticed that some Quaternary and Pliocene groundwater samples in periods 2016 and 2022 contain concentrations of lead that violate the drinking water guidelines (WHO, 2017). Extreme levels of lead absorption in the human body can cause death or perpetual harm to the brain, central nervous system, and kidneys (USGAO, 2000).

Several factors can explain the increasing concentrations of trace elements in the groundwater in the study area;

1- High trace elements such as iron and manganese in groundwater may be due to the dissolution process of the aquifer matrices.
2- The infiltration of contaminated irrigation canals water with liquid industrial wastes and agricultural activities into the groundwater, as well as the irrigation return water flow.
3- Seepage of wastewater from El Saff canal to the groundwater in the study area, where the population growth led to an increase in human activity, which in turn led to the use of El Saff canal for wastewater to irrigate the lands near El Saff canal for wastewater with its wastewater, which affected on the groundwater quality.

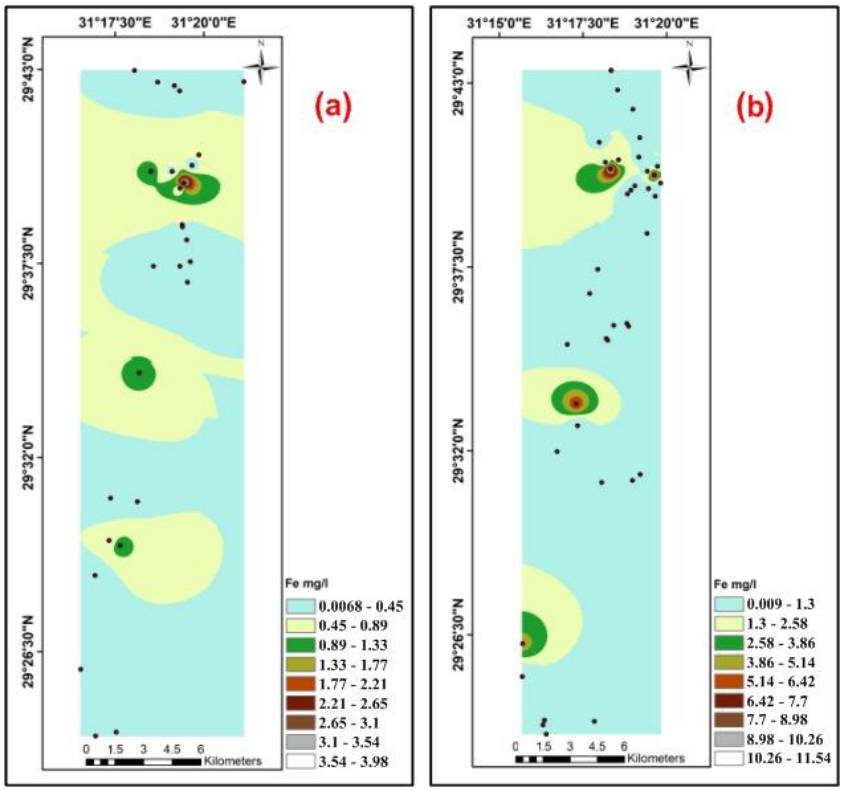

Fig. 33: Iron zonation contour map of the Quaternary groundwater in a (Period, 2016) and b (Period, 2022) in the study area

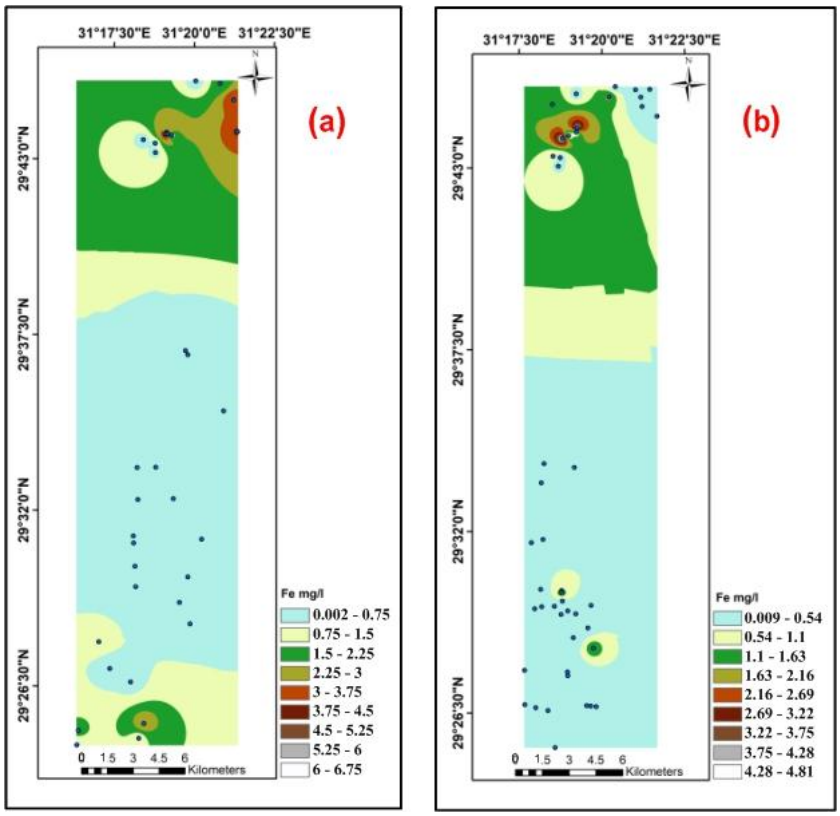

Fig. 34: Iron zonation contour map of the Pliocene groundwater in a (Period, 2016) and b (Period, 2022) in the study area

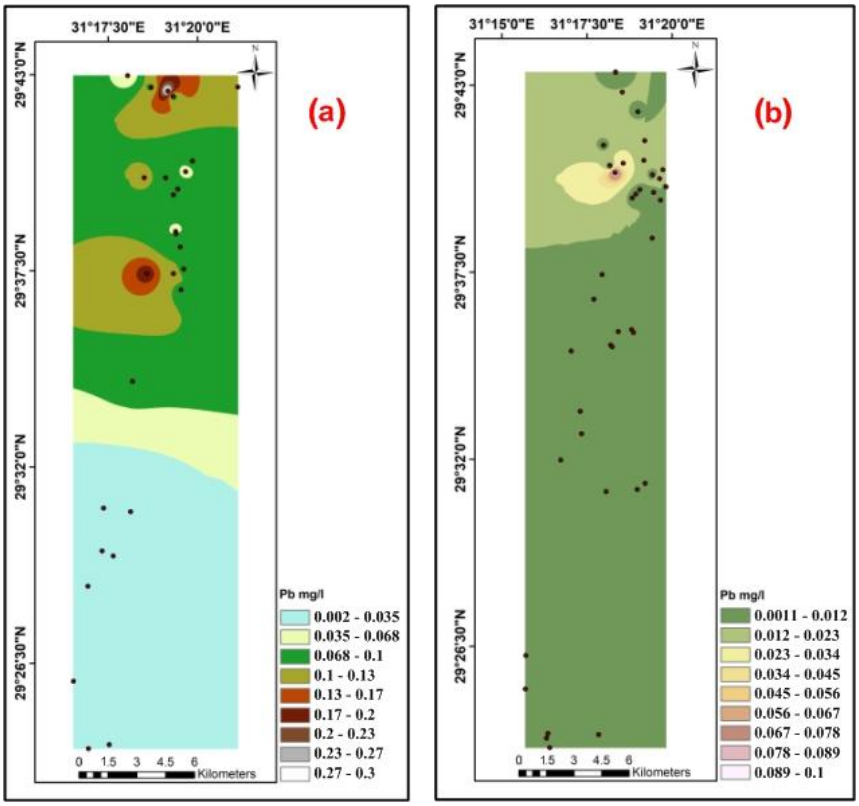

Fig. 35: Lead zonation contour map of the Quaternary groundwater in a (Period, 2016) and b (Period, 2022) in the study area

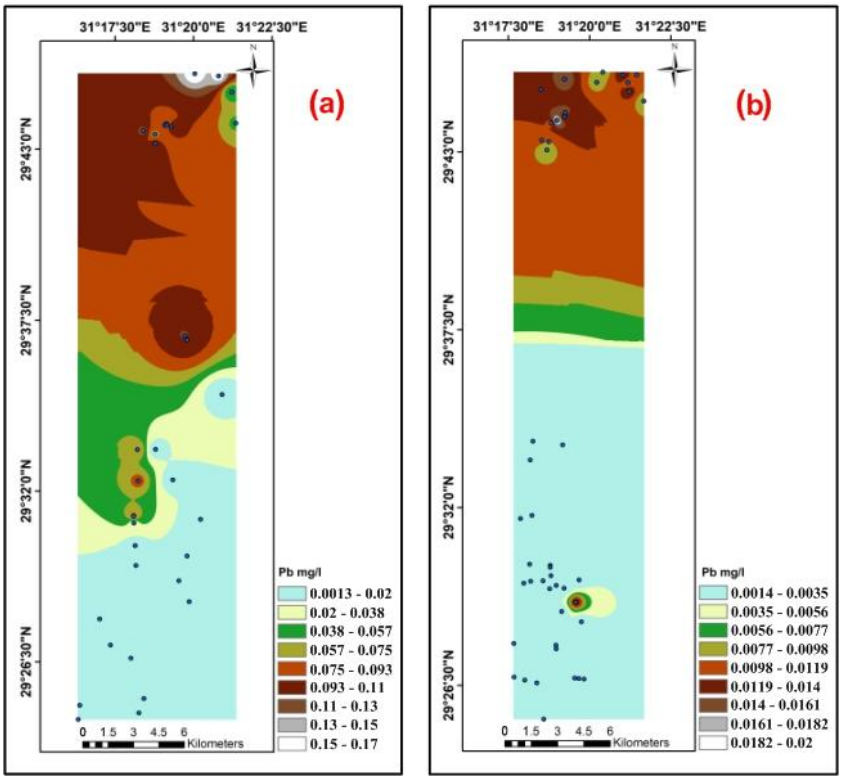

Fig. 36: Lead zonation contour map of the Pliocene groundwater in a (Period, 2016) and b (Period, 2022) in the study area

Table 9: The concentrations of trace and minor constituents in the Quaternary and Pliocene groundwater samples as mg/l (Period, 2016)

Statistics	Parameters									
	Al	**Cr**	**Cu**	**Fe**	**Mn**	**Ni**	**Zn**	**Pb**	**B**	**NO_3^-**
Quaternary groundwater samples										
Minimum	0.0034	0.0012	0.0017	0.0068	0.0004	0.0018	0.0021	0.0021	0.015	0.377
Maximum	1.558	0.0281	0.1036	3.835	0.5204	0.046	2.226	0.301	2.68	79.87
Average	0.1459	0.0079	0.0149	0.5196	0.0778	0.0046	0.199	0.071	0.67	34.93
Pliocene groundwater samples										
Minimum	0.0052	0.0012	0.001	0.002	0.0004	0.0013	0.0004	0.0013	0.0151	17.03
Maximum	1.323	0.0322	0.0525	6.729	0.5156	0.0708	2.226	0.1669	2.359	81.99
Average	0.1081	0.0084	0.0089	1.049	0.1227	0.0114	0.3529	0.0483	0.5473	48.19
Permissible limits	0.2	0.05	2	0.3	0.4	0.07	5	0.01	0.5	50

Table 10: The concentrations of trace and minor constituents in the Quaternary and Pliocene groundwater samples as mg/l (period, 2022)

Statistics	Parameters									
	Al	**Cr**	**Cu**	**Fe**	**Mn**	**Ni**	**Zn**	**Pb**	**B**	**NO_3^-**
Quaternary groundwater samples										
Minimum	0.003	0.0004	0.0007	0.009	0.0004	0.0004	0.0005	0.0011	0.052	2.1
Maximum	1.84	0.052	1.75	11.53	0.793	0.009	7.88	0.099	16.83	194
Average	0.0947	0.0069	0.0460	1.0031	0.0983	0.0009	0.5894	0.0074	3.221	55.49
Pliocene groundwater samples										
Minimum	0.0002	0.0004	0.0001	0.009	0.0003	0.0001	0.0004	0.0014	0.003	10.5
Maximum	1.39	0.326	0.351	4.8	2.62	0.036	8.94	0.0198	17.15	241.1
Average	0.0739	0.0168	0.0209	0.492	0.1377	0.0023	0.4663	0.0103	6.4523	102.7

Microbiological pollution

The microbiological pollution of a water resource in an area is investigated by measuring the total and fecal coliforms bacteria in this water resource. Total coliforms include bacteria that are found in the soil, in water that has been influenced by surface water, and in human or animal waste. Fecal coliforms are the group of the total coliforms that are considered to be present specifically in the gut and feces of warm-blooded animals. The presence of fecal contamination is a sign that a possible health risk exists for individuals exposed to this water (Ohio, 2004). The microbiological pollution of the surface water and groundwater in the study area was investigated by measuring the total and fecal coliforms bacteria in some selected surface water samples (irrigation canals, El Saff canal for wastewater) and groundwater samples (the Quaternary and Pliocene aquifers) collected during the two periods (2016 and 2022) especially for microbiological measurements to verify that this water is microbiologically polluted or not (tables 11 & 12). By comparing the analyses results data (tables 11 & 12) with WHO (2017) standards limits for drinking water (the drinking water must not contain any total or fecal coliform bacteria), it is clear that all selected surface water and groundwater samples that were collected from the study area were polluted with total and fecal coliform bacteria and the pollution increased by time from 2016 to 2022. This may be due to the following factors:

1- The effect of El Saff canal for wastewater on the surface water and groundwater in the study area is either by draining the wastewater directly into the River Nile (Fig. 14a) which in turn reaches the irrigation canals and is then recharged to the groundwater, or by seepage of the wastewater of El Saff canal into the groundwater through faults and clastics (Fig. 7).
2- The anthropogenic activities include the use of septic tanks that are occasionally disposed of in the irrigation canals because there are no good sewerage systems in most localities in the study area, i.e., the irrigation canals are sometimes used as drains (Fig. 14d).

Table 11: The total viable bacterial counts (TVBCs) x 10^4 cfu/ml water, the most probable number (MPN) of total coliforms (TC), in the surface water and groundwater at the study area (Period, 2016)

Parameters	Irrigation canals			El Saff canal for wastewater			Groundwater			WHO (2017)
	Min.	Max.	Average	Min.	Max.	Average	Min.	Max.	Average	
Total coliforms MPN/100ml	19	60	34	800	1300	1150	10	150	25	0
Fecal coliforms cfu /100ml	5	20	10	180	260	220	2	20	5	0

Table 12: The total viable bacterial counts (TVBCs) x 10^4 cfu/ml water, the most probable number (MPN) of total coliforms (TC), in the surface water and groundwater at the study area (Period, 2022)

Parameters	Irrigation canals			El Saff canal for wastewater			Groundwater			WHO (2017)
	Min.	Max.	Average	Min.	Max.	Average	Min.	Max.	Average	
Total coliforms MPN/100ml	10	275	196	900	1800	1542	30	920	425	0
Fecal coliforms cfu /100ml	20	83	50	310	390	309	3	440	234	0

Statistical analysis (cluster)

Cluster analysis is a group of multivariate techniques that primarily classify variables or cases (samples) into the cluster with a high homogeneity level within the class and a high heterogeneity level between classes (Massart and Kaufmann, 1983). So, the multivariate analysis techniques are important tools for assessing the hydrochemical characteristics of groundwater (Wali *et al.,* 2021). The cluster analysis (CA) was performed to identify groups of sites (clusters) exhibiting similar water chemistry because the cluster analysis (CA) uses the ward method, which its rule indicates that the shorter the distance between two data points, the greater the similarity between them.

Among the purposes of using cluster analysis in the current study is to detect the groundwater samples that were affected by the agricultural activities due to the return flow after irrigation and the anthropogenic influences due to the seepage from El Saff canal for wastewater on the hydrochemical characteristics of the groundwater during the two periods (2016 and 2022). Moreover, delineate the most deteriorated localities in the study area.

The results of the cluster analysis (Dendogram) for the samples are represented in Figs. (37 & 38) in period (2016) and in Figs. (39 & 40) in period (2022). In period (2016), the CA grouped 87 sampling locations into 2 clusters named 1 & 2, with 4 sub-clusters named A, B, C and D. While in period (2022), the CA grouped 104 sampling locations into 2 clusters named 1 & 2, with 4 sub-clusters named A, B, C and D, and sub-sub-clusters B_1 and B_2. Clusters of the samples in the two periods are listed in tables (13 & 14), respectively, which indicate that each cluster has a water quality of its own that is different from the other cluster.

In period (2016), cluster No.1 is represented by 21 surface water samples and 59 groundwater samples (table 13 and figures 37 & 38) and it is sub-divided into two sub-clusters named A and B. Sub-cluster (A) is represented by 18 surface water samples {El Hager canal (3 samples), El Khashab canal (2 samples), Masjid Musi canal (one sample) and El Saff canal for wastewater (12 samples)} and 35 groundwater samples {Quaternary aquifer (20 samples) and Pliocene aquifer (15 samples)}. While, sub-cluster (B) is represented by 3 surface water samples {El Hager canal (2 samples) and El Saff canal for wastewater (one sample)} and 24 groundwater samples {Quaternary aquifer (12 samples) and Pliocene aquifer (12 samples)}. It is noteworthy to mention that the groundwater samples in the cluster No.1 are distributed all over the study area (Fig. 38).

Moreover, cluster No.2 is represented by 7 groundwater samples (table 13 and figures 37 & 38) and it is sub-divided into two sub-clusters named C and D. Sub-cluster (C) is represented by 5 groundwater samples tapping the Pliocene aquifer, while sub-cluster (D) is represented by 2 groundwater samples {Quaternary aquifer (one sample) and Pliocene aquifer (one sample)}.

It is obvious that the sub-cluster (A) is the most sub-cluster in the study area that contains surface water samples (irrigation canals and El Saff canal for wastewater samples) located between the groundwater samples, which means that the groundwater samples in this cluster were highly affected by the agricultural activities due to the return flow after irrigation and the anthropogenic influences due to the seepage from El Saff canal for wastewater, which in turn affected on the hydrochemical characteristics of most groundwater (53%) in the study area in period 2016.

In period (2022), cluster No.1 is represented by 17 surface water samples and 81 groundwater samples (table 14 and figures 39 & 40) and it is sub-divided into two sub-clusters named A and B. Sub-cluster (A) is represented by 9 surface water samples {El Khashab canal (3 samples), Masjid Musi alqabliya canal (3 samples) and El Saff canal for wastewater (3 samples)} and 27 groundwater samples {Quaternary aquifer (20 samples) and Pliocene aquifer (7 samples)}. While, sub-cluster (B) is represented by 8 surface water samples and 54 groundwater samples and it is sub-divided into two sub-sub-clusters named B_1 and B_2. The sub-sub-cluster (B_1) is represented by 17 groundwater samples {Quaternary aquifer (4 samples) and Pliocene aquifer (13 samples)}. Whereas, the sub-sub-cluster (B_2) is represented by 8 surface water samples {El Hager canal (2 samples) and El Saff canal for wastewater (6 samples)} and 37 groundwater samples {Quaternary aquifer (17 samples) and Pliocene aquifer (20 samples)}. Noteworthy mention, the groundwater samples in the sub-cluster (A) and sub-sub-cluster (B_2) were distributed all over the study area (Fig. 40).

Moreover, cluster No.2 is represented by 6 groundwater samples tapping the Pliocene aquifer and it is sub-divided into two sub-clusters named C and D (table 14 and figures 39 & 40).

It is obvious that both the sub-cluster (A) and sub-sub-cluster (B_2) are the most sub and sub-sub-clusters in the study area that contain surface water samples (irrigation canals and El Saff canal for wastewater samples) located between the groundwater samples, which means that the groundwater samples in these clusters were highly affected by the agricultural activities due to the return flow after irrigation and the anthropogenic influences due to the seepage from El Saff canal for wastewater, which in turn affected on the hydrochemical characteristics of most groundwater (73%) in the study area in period 2022.

Table 13: Clusters groups and their members of the surface water and groundwater samples in the study area in period 2016

Clusters groups	Sub-clusters	Members (Samples Nos.)
1	A	El Hager canal (3, 4 & 5), El Khashab canal (6 & 7), Masjid Musi alqabliya canal (8), El Saff canal for wastewater (9, 10, 11, 13, 14, 15, 16, 17, 18, 19, 20 & 21), Quaternary aquifer (22, 24, 29, 32, 33, 34, 35, 36, 40, 41, 42, 43, 44, 45, 46, 47, 48, 49, 50 & 52), Pliocene aquifer (59, 60, 61, 63, 69, 70, 71, 75, 76, 77, 78, 79, 80, 83 & 84).
	B	El Hager canal (1 & 2), El Saff canal for wastewater (12), Quaternary aquifer (23, 25, 26, 28, 30, 31, 37, 38, 39, 51, 53 & 54), Pliocene aquifer (62, 64, 65, 67, 68, 72, 73, 74, 81, 82, 85 & 86).
2	C	Pliocene aquifer (55, 56, 57, 58 & 66).
	D	Quaternary aquifer (27), Pliocene aquifer (87).

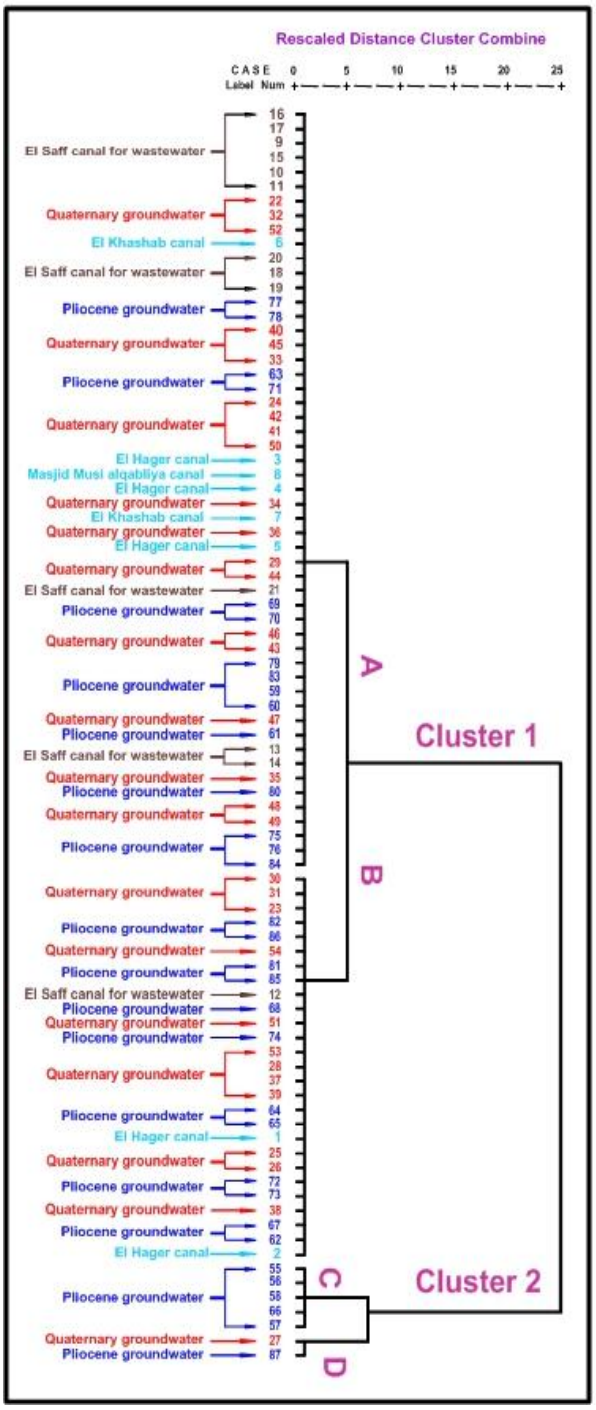

Fig.37: Dendogram of cluster analysis of both surface water and groundwater samples in the study area (Period, 2016)

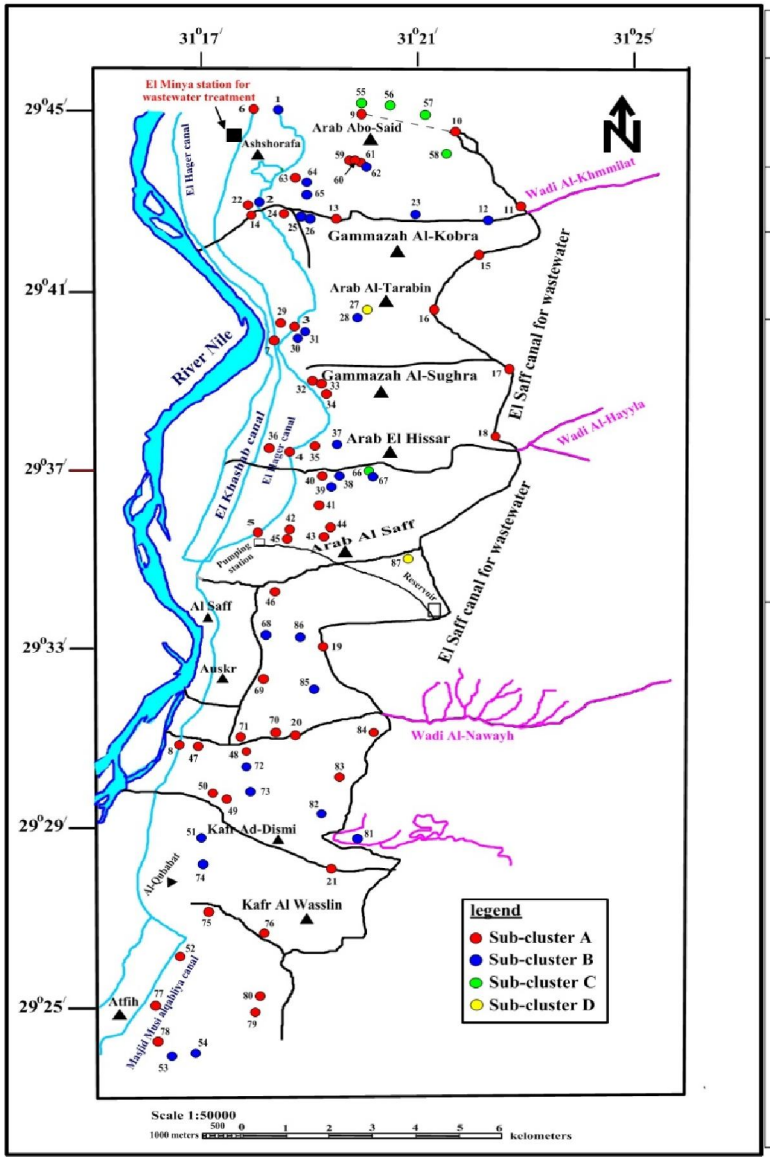

Water type	Sample No.	Water type	Sample No.
El Haoer canal	1	Quaternary aquifer	47
	2		48
	3		49
	4		50
	5		51
El Khashab canal	6		52
	7		53
			54
Masjid Musi alqabliya canal	8	Pliocene aquifer	55
			56
			57
			58
El Saff canal for wastewater	9		59
	10		60
	11		61
	12		62
	13		63
	14		64
	15		65
	16		66
	17		67
	18		68
	19		69
	20		70
	21		71
Quaternary aquifer	22		72
	23		73
	24		74
	25		75
	26		76
	27		77
	28		78
	29		79
	30		80
	31		81
	32		82
	33		83
	34		84
	35		85
	36		86
	37		87
	38		
	39		
	40		
	41		
	42		
	43		
	44		
	45		
	46		

Fig. 38: Sub-clusters distribution map of the surface water and groundwater in the study area (Period, 2016)

Table 14: Clusters groups and their members of the surface water and groundwater samples in the study area in period 2022

Clusters groups	Sub-clusters		Members (Samples Nos.)
1	A		El Khashab canal (4, 5 & 6), Masjid Musi alqabliya canal (7, 8 & 9), El Saff canal for wastewater (10, 13 & 16), Quaternary aquifer (23, 24, 25, 26, 27, 29, 30, 32, 36, 39, 40, 44, 45, 46, 47, 49, 51, 52, 53 & 54), Pliocene aquifer (68, 75, 76, 79, 101, 102 & 103).
	B	B1	Quaternary aquifer (22, 31, 33 & 34), Pliocene aquifer (60, 62, 71, 80, 81, 82, 83, 86, 87, 96, 97, 98 & 100).
		B2	El Hager canal (2 & 3), El Saff canal for wastewater (11, 12, 14, 15, 17 & 18), Quaternary aquifer (19, 20, 21, 28, 35, 36, 37, 38, 41, 42, 43, 48, 50, 55, 56, 57 & 58), Pliocene aquifer (65, 69, 70, 72, 73, 74, 77, 78, 84, 85, 88, 89, 90, 91, 92, 93, 94, 95, 99 & 104).
2	C		Pliocene aquifer (64 & 67).
	D		Pliocene aquifer (59, 61, 63 & 66).

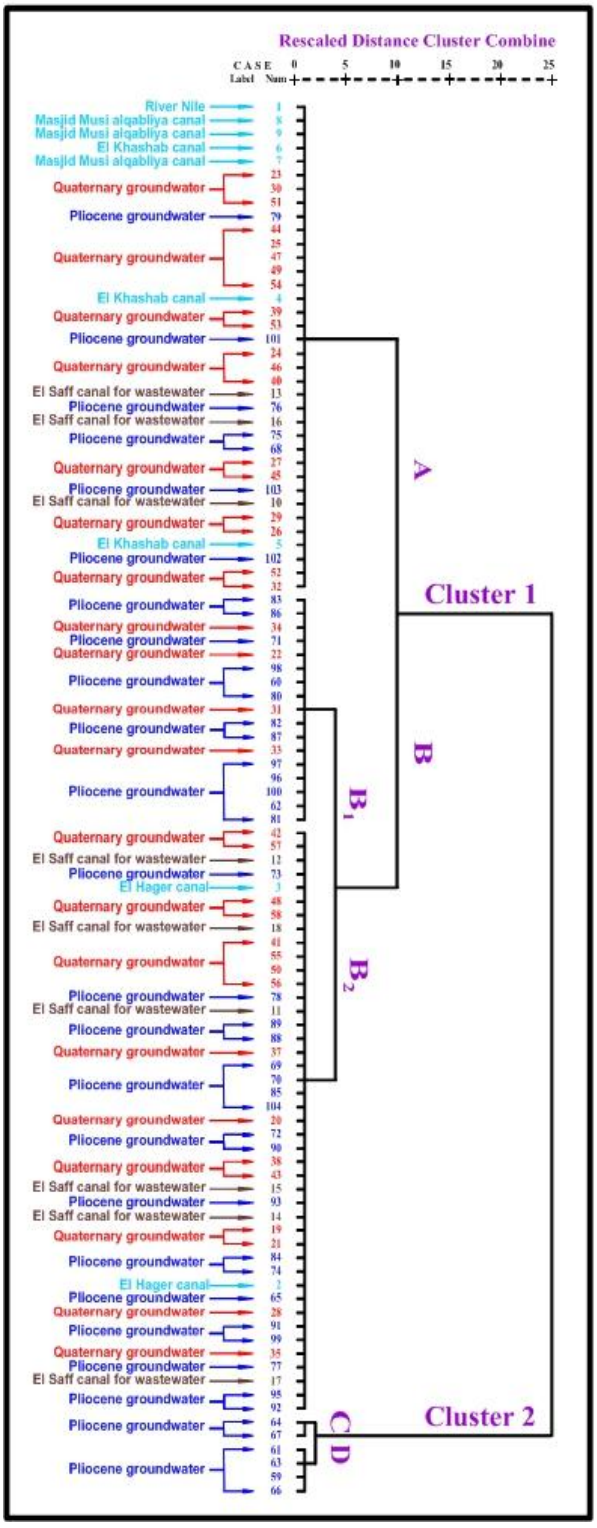

Fig. 39: Dendogram of cluster analysis of both surface water and groundwater in the study area (Period, 2022)

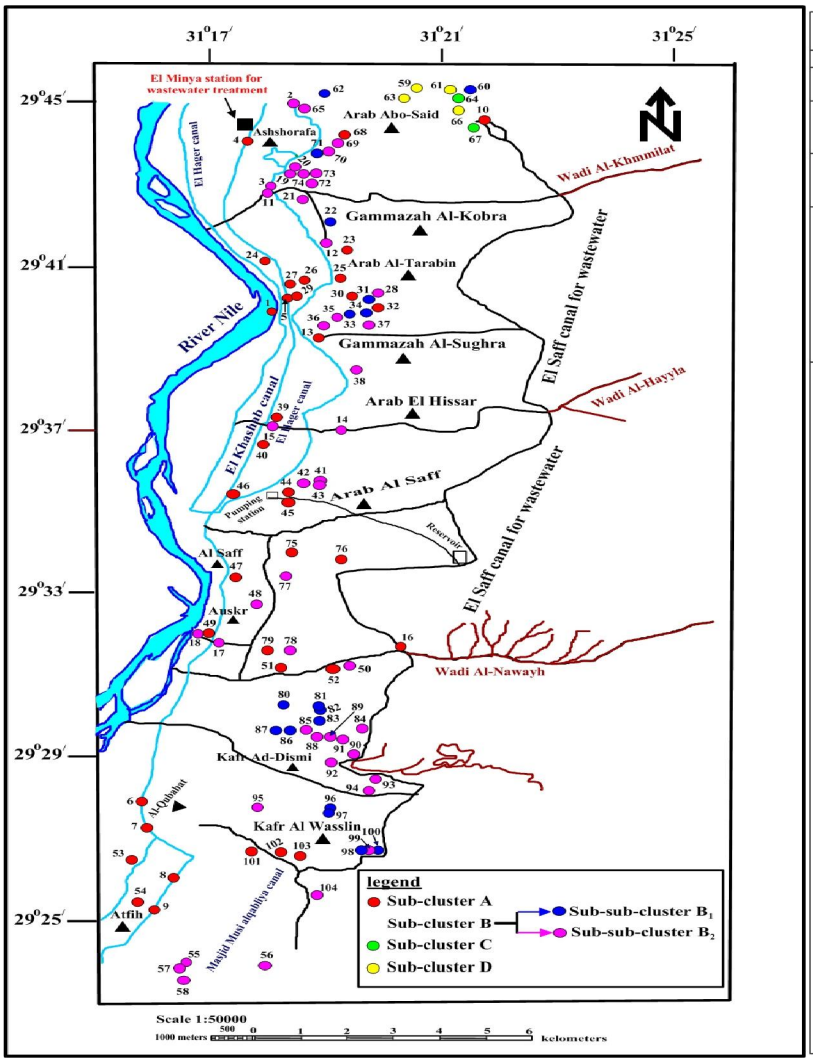

Water type	Sample No.	Water type	Sample No.
River Nile	1	Pliocene aquifer	59
El Hager canal	2		60
	3		61
El Khashab canal	4		62
	5		63
	6		64
Masjid Musi alqabliya canal	7		65
	8		66
	9		67
El Saff canal for wastewater	10		68
	11		69
	12		70
	13		71
	14		72
	15		73
	16		74
	17		75
	18		76
Quaternary aquifer	19		77
	20		78
	21		79
	22		80
	23		81
	24		82
	25		83
	26		84
	27		85
	28		86
	29		87
	30		88
	31		89
	32		90
	33		91
	34		92
	35		93
	36		94
	37		95
	38		96
	39		97
	40		98
	41		99
	42		100
	43		101
	44		102
	45		103
	46		104
	47		
	48		
	49		
	50		
	51		
	52		
	53		
	54		
	55		
	56		
	57		
	58		

Fig. 40: Sub-clusters distribution map of the surface water and groundwater in the study area (Period, 2022)

From the cluster analysis results, it can be concluded that:

1- The deteriorated groundwater samples in the study area increased by time from 53% (30% and 23% of Quaternary and Pliocene aquifers, respectively) in period 2016 to 73% (43% and 30% of Quaternary and Pliocene aquifers, respectively) in period 2022.

2- The quaternary aquifer is more deteriorated than the Pliocene one.

3-The most deteriorated localities in the study area are Arab Abo-Said, Arab Al-Tarabin, Arab Al-Saff, Auskr, Kafr Ad-Dismi and Kafr Al Wasslin.

Suitability of the water resources in the study area for human drinking

To assess the suitability of surface water (El Hager, El Khashab and Masjid Musi alqabliya canals) and groundwater (Quaternary and Pliocene aquifers) for drinking purposes in the two periods (2016 and 2022), the analyses results were compared with the international standards of drinking water (WHO, 2017). Where, the drinking water standards of TDS according to WHO (2017) is 1000mg/l. So, in period 2016, the majority of the irrigation canals water samples (75%) and a minority of the groundwater samples (23%) in the study area are suitable for human drinking, while the rest of the irrigation canals water samples (25%) and the majority of the groundwater samples (75%) in the study area are unsuitable for human drinking as they exceed the allowable limit of 1000mg/l (Fig. 41). In period 2022, 60% of the irrigation canals water samples and 16% of the groundwater samples in the study area are suitable for human drinking, while the rest of the irrigation canals water samples (40%) and the majority of the groundwater samples (84%) in the study area are unsuitable for human drinking as they exceed the allowable limit 1000mg/l (Fig. 42). Also, it is clear that the majority of the irrigation canals water samples and the groundwater samples in the study area are unsuitable for human drinking as they have iron, boron and nitrate concentrations higher than the permissible limits (WHO, 2017). From the aforementioned, it can be concluded that the suitability of surface water and groundwater for human drinking in the study area decreased by time from 2016 to 2022 (Figs. 41 & 42).

Suitability of the water resources in the study area for irrigation

Water quality assessment is very important for guiding farmland irrigation processes. In this study, the EC and SAR index values were included in order to assess the irrigation water quality. So, when surface water and groundwater are used for irrigation, both salt and alkali hazards must be considered. A large amount of salt enters farmland with irrigation water, causing crop yield reduction and soil salinization to intensify (Jassas and Merkel, 2015). The most useful parameter for determining the suitability of groundwater for irrigation purposes is the sodium adsorption ratio (SAR) values, because SAR is an important indicator of sodium hazards, where if the value of SAR is too large, this will harm the permeability and structure of the soil (Tang *et al.,* 2019). The USSL diagram (Staff, 1954) takes EC as the abscissa and SAR as the ordinate. The EC represents salt damage, and the SAR represents alkali damage.

According to the USSL diagrams as in Fig. 43(a & b), we can conclude that;

1- 76%, 27% and 22% of the irrigation canals, Quaternary groundwater and Pliocene groundwater samples, respectively, in period 2016 (Fig. 43a), as well as 74%, 19% and 17% of the irrigation canals, Quaternary groundwater and Pliocene groundwater samples, respectively, in period 2022 (Fig. 43b), are good water and considered suitable for the irrigation of majority plants for all soils.
2- 12%, 41% and 63% of the irrigation canals, Quaternary groundwater and Pliocene groundwater samples, respectively, in period 2016 (Fig. 43a), as well as 11%, 31% and 46% of the irrigation canals, Quaternary groundwater and Pliocene groundwater samples, respectively, in period 2022 (Fig. 43b), are unsuitable for irrigation under ordinary conditions but may be used occasionally under special conditions as if special soil management is taken into consideration, such as good drainage.
3- 12%, 40% and 15% of the irrigation canals, Quaternary groundwater and Pliocene groundwater samples, respectively, in period 2016 (Fig. 43a), as well as 15%, 42% and 37% of the irrigation canals, Quaternary groundwater and Pliocene groundwater samples, respectively, in period 2022 (Fig. 43b), are bad water and they are unsuitable for irrigation under ordinary conditions but may be used occasionally under special conditions as the irrigation water must be applied in excess to provide considerable leaching.

In conclusion, the surface water and groundwater quality in the study area are changing from period 2016 to period 2022, as they are ranging from good water to moderate water to bad water. It is noteworthy to mention that the good water quality of the surface water and groundwater samples in the study area decreased by time from period 2016 to 2022. While the bad water quality increased by time from period 2016 to 2022.

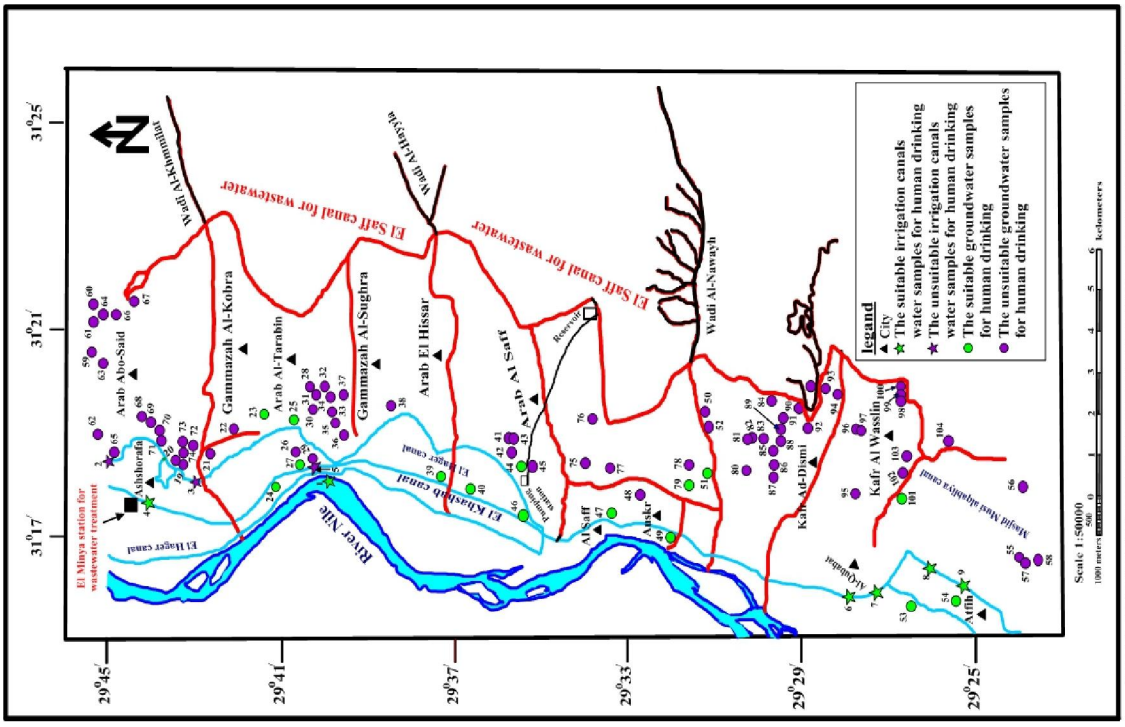

Fig.42 The suitability map of the irrigation canals water and groundwater samples in the study area for human drinking purpose (Period, 2022)

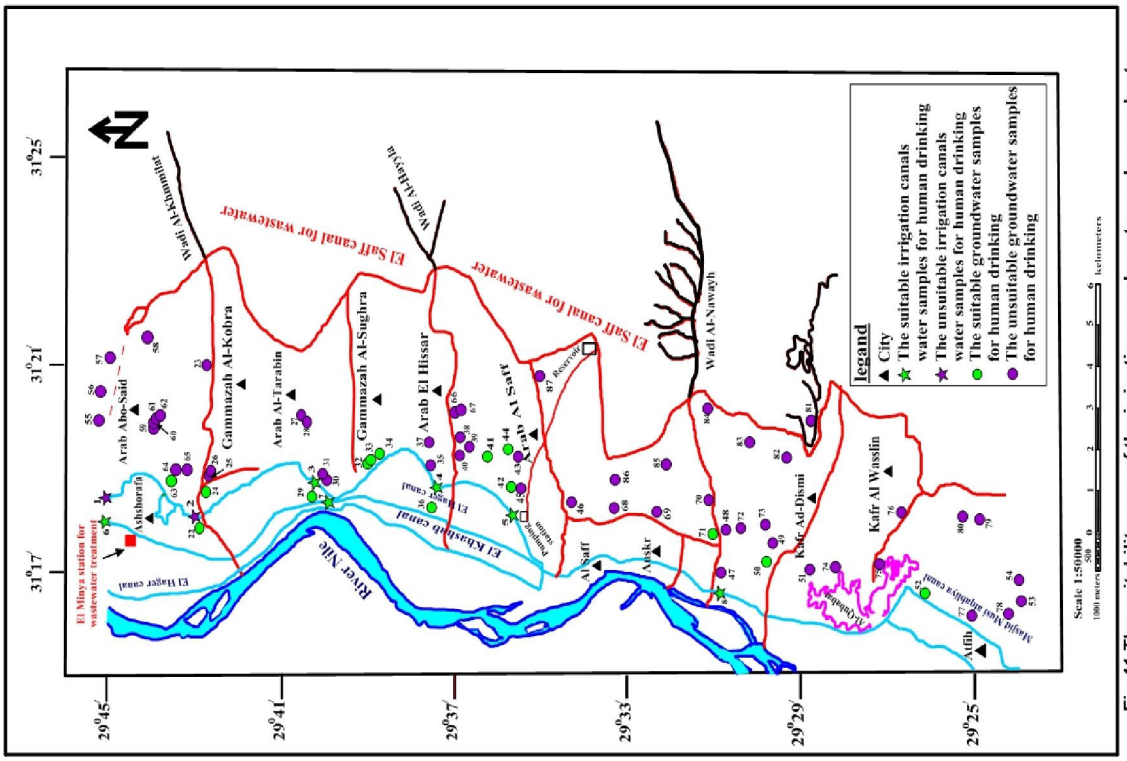

Fig.41 The suitability map of the irrigation canals water and groundwater samples in the study area for human drinking purpose (Period, 2016)

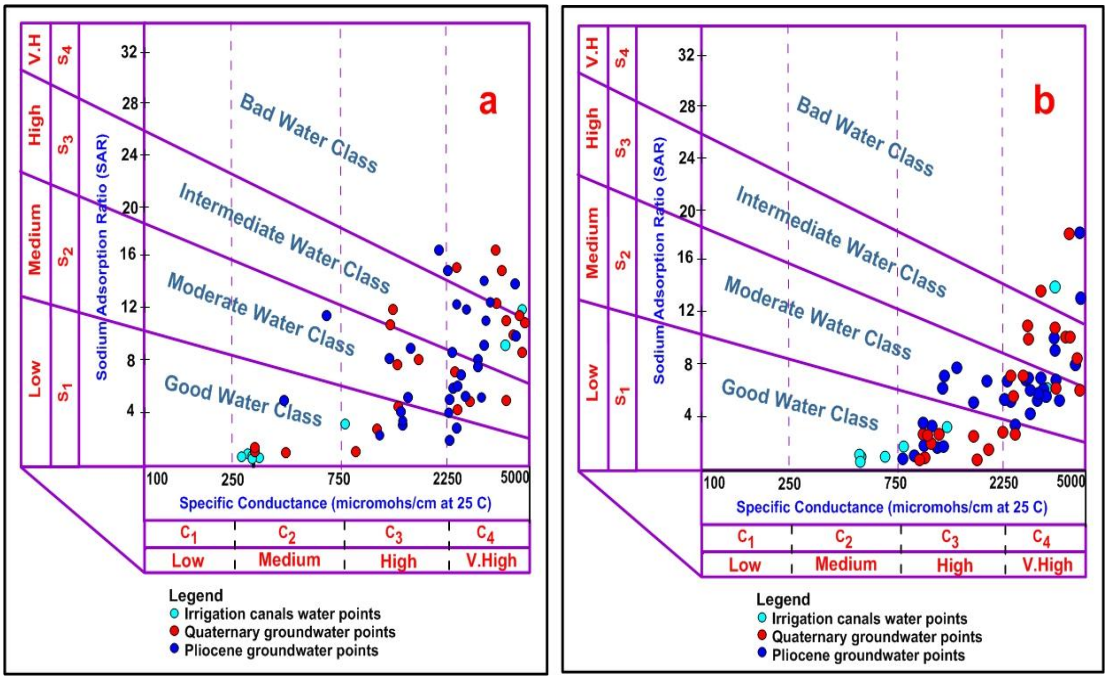

Fig. 43: U.S. Salinity Laboratory Staff (USSL) diagrams for the irrigation canals water samples and Quaternary as well as Pliocene groundwater samples in the study area in a (period, 2016) and b (period, 2022)

4. Conclusion

Integration between the chemical and microbiological data, statistical analyses, remote sensing and GIS techniques, in addition to geochemical modeling and Piper diagram as well as staff diagram was done to study the deterioration of the Quaternary and Pliocene groundwater quality in the area between El Saff and El Khashab canals. The present work clarifies that the main problem is the seepage of the wastewater of El Saff canal into the Quaternary and Pliocene groundwater, as well as the return flow after irrigation in the study area.

It was noticed that the salinity of El Saff canal for wastewater increased from period 2016 to period 2022. This may be due to the amounts of wastewater, polluted materials, harmful chemicals and garbage that were thrown from factories, agricultural lands, and cities into El Saff canal for wastewater, as well as, the fact that El saff canal was generally dug in the Pliocene clay sediments and sometimes cut the foot slope of the eastern limestone plateau.

The salinity of the irrigation canals water increases from south to north, and this relatively high salinity may be due to the effects of location, direction of water movement, type of soil, type of mixing source, rate of evaporation, and the drainage of some industrial factories, as well as the drainage of El Saff canal for wastewater into the River Nile as in El Ghammazah area, which moves again to the canals, and finally, in some areas, the irrigation canals are used as a drain. Also, it was clear that the salinity as well as the nitrate, boron, iron, manganese and lead concentrations in the irrigation canals water samples increased by time from 2016 to 2022, which indicates that the deterioration of the irrigation canals increased by time.

The groundwater salinity of the Quaternary and Pliocene aquifers in the concerned area increased by time from 2016 to 2022, and this may be due to the effect of seepage of El Saff canal for wastewater during faults (anthropogenic activity) as well as return flow after irrigation (agricultural activities), in addition to the over pumping. Also, the interaction between the groundwater and the geological formations and the leaching of soil processes due to the increase in groundwater extraction to meet the agricultural activities in the new reclamation areas, as well as the ion exchange processes that occurred on the clay surface, which constitute the main cause of the high salinity. Consequently, this leads to the deterioration of the groundwater by time from 2016 to 2022.

The high concentrations of nitrate, boron, iron, manganese and lead in the groundwater in the study area increase by time, and this could be attributed to contamination from the released wastewater and irrigation water return flow. This means that the effect of El Saff canal for wastewater on the groundwater in the study area increased by time from 2016 to 2022. Consequently, the groundwater in the study area became more polluted and in turn, deteriorated by time.

The Piper diagram and geochemical model, as well as statistical analyses confirmed that both the Quaternary and Pliocene groundwater deteriorated by time from 2016 to 2022, while the percentage of the groundwater samples that affected by El Saff canal for wastewater increased by time from 2016 to 2022.

It was clear that the majority of the groundwater samples in the study area were unsuitable for human drinking. Also, the percentage of good groundwater for human drinking and irrigation decreased with time from 2016 to 2022.

Recommendations

1- Stopping the drain of wastewater of El Saff canal (which contains a variety of pollutants) into the River Nile.
2- Stopping the use of wastewater of El Saff canal in irrigating the new reclaimed areas in the east of the study area.

Acknowledgments

The author greatly thanks Prof. Dr. Mohamed Yousif, professor and head of the geology department at the Desert Research Center, who has helped me in the application of remote sensing and GIS techniques.

References

Abdel-Daiem A.A., 1971. Hydrogeological studies of springs in the area to the east of Cairo. M.Sc. Thesis, Ain Shams Univeristy, 120.

Abdou I.I., 1994. Geology and hydrogeology of the Helwan area, Egypt. M.Sc. thesis, Menofia Univeristy, Egypt, 151.

American Society for Testing and Materials (ASTM), 2002. Water and environmental technology. Annual book of ASTM standards, Sec.11, Vols.11.01 and 11.02, West Conshohocken, U.S.A.

American Public Health Association (APHA), 1998. Standards methods for the examination of water and wastewater. 20thed., New York, U.S.A.

Anderson D.M., P.M. Glibert and J.M. Burkholder, 2002. Harmful algal blooms and eutrophication: nutrient sources, composition and consequences. Estuaries 25:704–726.

Anim-Gyampo M., G.K. Anornu, E.K. Appiah-Adjei and S.K. Agodzo, 2018. Hydrogeochemical evolution and quality assessment of groundwater within the Atankwidi basin: the case of northeastern Ghana. Arabian Journal of Geosciences, 11: 439.

Awad S.R., 2019. Groundwater hydrogeology and quality in Helwan area and its vicinities in Egypt. Scientific Journal of National Water Research Center (NWRC), 33(1):10-21.

Bahir M., S. Ouhamdouch, D. Ouazar and A. Chehbouni, 2020. Assessment of groundwater quality from semi-arid area for drinking purpose using statistical, water quality index (WQI) and GIS technique. Carbonates and Evaporites., 35(1):1–24.

Barzegar R., A.A. Moghaddam, E. Tziritis, M.S. Fakhri and S. Soltani, 2017. Identification of hydrogeochemical processes and pollution sources of groundwater resources in the Marand plain, northwest of Iran. Environ. Earth Sci., 76(7): 297.

Bohlke J.K., 2002. Groundwater recharge and agricultural contamination. Hydrogeol. J., 10:153–179.

Chebotarev I.I., 1955. Metamorphism of natural waters in the crust of weathering. Geochim. Cosmochim. Acta, 8: 22-212.

CONOCO, 1987. Geological map of Egypt, scale 1:500000, sheet No. N. H. 36 SW BeniSuef. The Egyptian General Petroleum Corporation.

Deutsch W.J. and R. Siegel, 1997. Groundwater geochemistry: fundamentals and application to contamination. CRC, Roca.

Egypt Census estimation, 2017. Estimation of Central Agency for Public Mobilization and Statistics (in Arabic).

Egypt Census estimation, 2023. Estimation of Central Agency for Public Mobilization and Statistics (in Arabic).

El Gaby S.A.A., 2020. Environmental hydrogeological study using remote sensing and GIS at Helwan district, Egypt. Ph.D. Thesis, Geology department, Faculty of Science, Helwan University, 207p.

El Kadi A.I., N.L. Plummer and P. Aggarwal, 2010. NETPATH-WIN: an interactive user version of the mass-balance model, NETPATH. Department of Geology and Geophysics and Water Resources Research Center, University of Hawaii at Manoa, Honolulu, Hawaii 96822(808):956–6331.

El-Sayed, E.E.S., 1993. Hydrogeological Studies of the Nile Valley in the Northern Portion of Upper Egypt. Ph.D. Thesis. Fac. Sci. El-Minia Univ., Egypt.

El-Sayed S.A., S.M. Morsy and K.M. Zakaria, 2018. Recharge sources and geochemical evolution of groundwater in the Quaternary aquifer at Atfih area, the northeastern Nile Valley, Egypt. Journal of African Earth Sciences, 142: 82-92.

ElSheikh A.E., 2008. Hydrological assessment of the waterlogging problem in El Saff-Atfih area, southeast Cairo, Egypt. Assiut Univ. J. of Geology, 37(2):159-188.

Egyptian Higher Committee for Water, 2007. Water quality guidelines for human drinking, domestic and laundry uses, Egypt (in Arabic).

EMA (Egyptian Meteorological Authority), 1996. Climatic Atlas of Egypt. Egyptian Meteorological Authority, Ministry of Transport and Communications, Cairo, Egypt.

Fan A.M. and V.E. Steinberg, 1996. Health implications of nitrate and nitrite in drinking water: An Update on Methemoglobinemia occurrence and reproductive and developmental toxicity: Regulatory Toxicology and Pharmacology, 23:35-43.

Fishman M.J. and L.C. Friedman, 1985. Methods for determination of inorganic substances in water and fluvial sediments. U.S. Geol. Surv. Book 5, Chapter A1. Open File Report, 85-495, Denver, Colorado, U.S.A.

Gu B., J. Park and P. Konana, 2012. Research Note: The impact of external word-of-mouth sources on retailer sales of high-involvement products. Information Systems Research, 23(1): 182–196.

Hem J.D., 1993. Factors affecting stream water quality, and water-quality trends in four basins in the conterminous United States 1905-90. In: Paulson RW, Chase EB, Williams JS, Moody DW (eds) National water summary 1990-91; hydrologic events and stream water quality. USGS water supply paper, 2400:67–92.

Hobbs W.H., 1904. Lineaments of the Atlantic Border region. Bull. Geol. Soc. Am., 15: 483–506.

Hobbs W.H., 1912. Earth Features and Their Meaning: An Introduction to Geology for the Student and General Reader, Macmillan, New York, N.Y., 347p.

Jassas H., and B. Merkel, 2015. Assessment of hydrochemical evolution of groundwater and its suitability for drinking and irrigation purposes in Al-Khazir Gomal basin, northern Iraq. Environmental Earth Sciences, 74(9): 6647–6663.

Jeong C.H., 2001. Effect of land use and urbanization on hydrochemistry and contamination of groundwater from Taejon area. Korea. J. Hydrol., 253 (1-4): 194–210.

Korany E.A., M.M. El-Ghazawi and B.J. Faiad, 1997a. Hydrographic analysis and hydrogeologic bearing of Wadi El-Atfihy, Eastern Desert, Egypt-a case study of an ephemeral stream. Ain Shams Sci. Bul., 35: 73-88.

Li J., S.Z. Zou, Y. Zhao, R.K. Zhao, Z.W. Dang, M.Q. Pan, D.N. Zhu and C.S. Zhou, 2021. Major ionic characteristics and factors of Karst groundwater at Huixian Karst Wetland, China. Environmental Science, 42(4):1750-1760.

Li P., S. He, X. He and R. Tian, 2018a. Seasonal hydrochemical characterization and groundwater quality delineation based on matter element extension analysis in a paper wastewater irrigation area, northwest China. Expo. Health, 10: 241–258.

Massar D.L. and L. Kaufman, 1983. The interpretation of chemical data by the use of cluster analysis. Wiley, New York.

Ohio, 2004. Ohio Department of Health, Bureau of Environmental Health, Private Water Program.

Panno S.V., K.C. Hackley, H.H. Hwang and W.R. Kelly, 2001. Determination of the sources of nitrate contamination in karst springs using isotopic and chemical indicators. Chem Geol 179(1-4):113–128.

Perera T.A.N.T., H.M.M.S.D. Herath, R.U.K. Piyadasa, L. Jianhui and L. Bing, 2022. Spatial and physicochemical assessment of groundwater quality in the urban coastal region of Sri Lanka. Environ. Sci. Pollut. Res., 29, 16250–16264.

Piper A.M., 1944. A graphic procedure in the geochemical interpretation of water-analyses, Eos. Transactions American Geophysical Union, 25(6); 914–928.

Rainwater F.H. and L.L. Thatcher, 1960. Methods for collection and analysis of water samples. U.S. Geol. Surv. Water Supply. Paper No.1454, U.S.A., 301.

Said R., 1954. Remarks on the geomorphology of the area east of Helwan. Bulletin of Society and geography of Egypt, 27:93-100.

Said K.F., 1962. Groundwater studies of Wadi El Natrun area and its vicinities. International report, Desert Institute, Cairo, Egypt.

Said R., 1981. The geological evolution of the Nile River. Springer Verlag, New York, 151.

Shankar B.S., N. Balasubramanya and M.M.T. Reddy, 2008. Impact of industrialization on groundwater quality—a case study of Peenya industrial area, Bangalore. Environ Monit Assess 142:263–268.

Tang J.P., Q. Zhang, Y. Hu, Y. Zhang and B.W. Nie, 2019. Groundwater chemical characteristics and analysis of their controlling factors in an alluvial fan of Jianjiang River. Environmental Science, 40(7): 3089-3098 (In Chinese).

USGAO, 2000. Health effect of lead in drinking water: U.S. General Accounting Office reports.

United States Salinity Laboratory Staff (USSL), 1954. Diagnosis and Improvement of Saline and Alkali Soils Department of Agriculture. US Handbook 60

Wali S.U., N. Alias and S.B. Harun, 2021. Reevaluating the hydrochemistry of groundwater in basement complex aquifers of Kaduna Basin, NW Nigeria using multivariate statistical analysis. Environ. Earth Sci., 80, 208.

Ward J.H. Jr., 1963. Hierarchical grouping to optimize an objective function. J Am Stat Assoc., 58:236–244

Wasserman G.A., X. Liu, F. Parvez, H. Ahsan, D. Levy, P. Factor-Litvak, J. Kline, A. van Geen, V. Slavkovich, N.J. LoIacono and Z. Cheng, 2006. Water manganese exposure and children's intellectual function in Araihazar, Bangladesh. Environ. Health Perspect. 114 (1): 124-129.

Wei A., Y. Chen, Q. Deng, D. Li, R. Wang and Z. Jiao, 2022. A study on hydrochemical characteristics and evolution processes of groundwater in the coastal area of the Dagujia River Basin, China. Sustainability, 14: 8358.

Weyer C., T. Funahashi, S. Tanaka, K. Hotta, Y. Matsuzawa, R.E. Pratley and P.A. Tataranni, 2001. Hypoadiponectinemia in obesity and type 2 diabetes: close association with insulin resistance and hyperinsulinemia. The journal of clinical endocrinology and metabolism, 86(5):1930-1935.

WHO, 2017. Guidelines for Drinking-water Quality: Fourth Edition Incorporating the First Addendum. WHO Library Cataloguing-in-Publication Data, Geneva.

WHO, 2021. Manganese in drinking-water. Background document for development of WHO Guidelines for drinking-water quality.

Xu P.P., W.W. Feng, H. Qian and Q.Y. Zhang, 2019. Hydrogeochemical characterization and irrigation quality assessment of shallow groundwater in the central-western Guanzhong Basin, China. International Journal of Environmental Research and Public Health, 16: 1492p.

Yang J.Y., B. Zhang, Y.F. Wu, Y. Feng, Y. Zheng and B.X. Shi, 2019. Balance between construction and conservation: strategy in water sensitive area planning. Applied ecology and environmental research, 17(4): 7283-7299.

Yousef A.F., 2007. Geology of groundwater resources in the reclaimed areas north of El Saff, Eastern desert, Egypt. E. J. of Desert Research, Matariya, Cairo, Egypt, 57(1):125-148.

Zhang Y.M., J. Zheng, T.R. Gaunt, H. Zhang, 2021. Mendelian randomization analysis reveals a causal effect of urinary sodium/urinary creatinine ratio on kidney function in Europeans Front. Bioeng. Biotechnol., 8:662.